ASSOCIATION BETWEEN MADDEN-JULIAN OSCILLATIONS AND WET AND DRY SPELLS OVER RWANDA

By

Joseph Ndakize SEBAZIGA

I45/69931/2013

Department of Meteorology

University of Nairobi

P.O.Box 30197

Nairobi

PROJECT SUBMITTED IN PARTIAL FULFILLMENT OF THE REQUIREMENTS FOR POST GRADUATE DIPLOMA IN METEOROLOGY OF THE UNIVERSITY OF NAIROBI

JULY, 2014

DECLARATION

This dissertation is my original work and has not been presented for a degree in any other University.

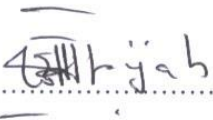Signature ....date.. 11|8|2014 .....

Joseph Ndakize SEBAZIGA

I45/69931/2013

This dissertation has been submitted for examination with our approval as University Supervisor

Signature ....date.. 11|8|2014 .....

Dr. Joseph N MUTEMI

Signature ....date.. 11|8|14 .....

Dr. Franklin J OPIJAH

Department of Meteorology

University of Nairobi

P.O Box 30197

Nairobi

DEDICATION

This project is dedicated to the entire members of my family for their endless support and encouragement throughout my education period: my wife NYIRASHIMWE Solange, my parents RUGABIRE K.Adrien and NYIRARUKUNDO Catherine , my brothrs; NGOGA Jonas, NDAYISHIMIYE Emmanuel NDATIMANA David, BAKAMA Didier and my sister; UMUTONI Diane.

ACKNOWLEDGEMENTS

ABSTRACT

The objective of this study was to examine the association between the Madden-Julian Oscillation (MJO) and wet and dry spells over Rwanda. Daily rainfall records and MJO indices was used in the study. The choice of daily MJO indices from 1979 to 2013 is based on the continuity of data as opposed to data from 1794, which has some missing data in 1978 and the choice of daily rainfall data from 1979 to 2013 was choosen to reflect the MJO indices. The methods used include temporal and spacial analysis, frequency analysis, correlation analysis and composite analysis.

The temporal and spatial analyses indicated that the rainfall peaks during the firts two weeks of March, which is the start month of the long rainfall season, starting from the western and southern part then to northern, central and estern part with high rainfall over the southern and western part of the country. This may be attributed to the westerly wind which inject moisture from Congo basin and the west fluctuation of the meridional arm of the ITCZ. The highlands of these regions also enhance convective development through orographic lifting.

The considerable number of wet spells during MAM season occurred between the third week of March and the second week of May while dry spells were located within the last two weeks of May. Composite of rainfall MJO indicated a well-established positive pattern between rainfall and wind component at lag zero and an opposite pattern between the rainfall and the Outgoing Long wave Radiation (OLR) component at the fifth lag.

The degree of association between MJO indices with daily rainfall was found to be moderately significant. The highest variance of daily rainfall explainable by Realtime Multivariate MJO principal component 2 (RMM2) indices is 25% while Realtime Multivariate MJO principal component 1 (RMM1) indices could explain a variance of16.8%.

TABLE OF CONTENTS

LIST OF FIGURES

LIST OF TABLES

CHAPTER ONE

1.0 INTRODUCTION

1.1 Background

Rwanda is located within the equatorial belt; its climate is, strictly speaking, not of the equatorial rain forest type. It has a modified humid climate including rain forest and Savannah. The central and eastern part of the country is generally of semi-arid type owing to its position in the rainy shadow of the western highlands.

Floods, landslides, and drought episodes constitute the major repetitive natural disasters for Rwanda and are often linked with ENSO episodes. Rwanda suffered serious floods linked to the ElNiñ0 episode of 1997/98 which destroyed a large number of agricultural plantations and ecosystems occupying the swamps of Nyabarongo and Akanyaru river basins. Prolonged drought of 1999 to 2000 seriously affected Bugesera. Landslides are common in the North (Gakenke, Cyeru, Rulindo, Butaro, and Kinihira) and the West (Nyamasheke, Karongi and Ngororero) of the country, including those that occurred in THE PERIOD 2001/2002.

Agriculture is the mainstay of the economy, contributing up to 80% of the Gross Domestic Product (GDP) OF RWANDA. The majority of the population practice subsistence farming but some parts is under extensive farming.

The impact of floods and droughts associated with El Nino and La Nina events of recent years are thought to have been caused by climate change and the poor environmental conditions suffered in the country identified in the (NAPA, 2006).

1.2 Statement of the Problem

Rainfall is the most important weather parameter that affects socio-economic activities over Rwanda. It affects almost all sectors of the economy such as agriculture, forestry, hydropower production, transport, water supply and human settlement among others. These activities are highly affected by intra-seasonal rainfall variability, which occurs within the season. There have been shortcomings in the rainfall prediction over Rwanda on intra-seasonal timescales. It is expected that the accuracy of rainfall prediction on these timescales may improve if the

association of rainfall variability over Rwanda with intra-seasonal oscillation, namely the Madden-Julian Oscillation (MJO), is established. MJO has well defined wave properties and knowledge of its linkage with wet/dry spells over Rwanda can directly help in weather predictability within the intra-seasonal time scale.

1.3 Objectives

The main objective of this study is to determine the association between the Madden-Julian Oscillations and wet and dry spells over Rwanda during the March to May season.

To help me achieve the main objective the following specific objectives were pursued:

1. To determine the temporal and spatial variability of rainfall based on daily rainfall over Rwanda during the March-May season

2. To assess the frequencies of wet and dry spells over Rwanda based on daily rainfall during the March-May season

3. To determine the associatioin between rainfall and the Madden-Julian Oscillation during the March-May season on a daily basis.

1.4 Hypothesis of the Study

Rainfallvariability on intra-seasonal timescales over Rwanda is assocaited with the pattern of Madden-Julian Oscillations over the region.

1.5 Justification of Study

Information on rainfall is important in order to ensure food security of the country that depends on the rain-fed agriculture. Accurate prediction and early warning of the expected rainfall extremes are critical for sustainable development of Rwanda. Most predictions of rainfall in the country focus on seasonal and short range forecasts for operational use and deterministic Numerical Weather Prediction (NWP) based on daily changes in pressure, wind and relative humidity provide useful skill out to six days. This leaves a gap between the medium range and seasonal forecasts, hence the need to fill the gap through intra-seasonal prediction. MJO can be a useful predictor because it is a migratory system and its progression characteristics can be used to indicate the likely occurrence of wet and dry spells.

1.6 Area of Study

Rwanda is a landlocked country located in Central and Eastern Africa, bordered by the Democratic Republic of Congo (DRC) to the West, Uganda to the North, Tanzania to the East and Burundi to the South. It lies within $1^0 - 3^0$ South of the equator and longitude $28^0 - 31^0$ E.

Rwanda has two major rain seasons in a year; the first season runs from March to May and the second one runs from September to December. These are separated by two dry seasons; the major dry season is from June to August and the shorter one running from December to February. Rainfall varies geographically, with the western and North-Western regions of the country receiving more precipitation annually than the Central, Eastern and South-eastern regions.

Figure 1: The study site (Republic of Rwanda)

Some of the main factors that influence rainfall over Rwanda include: The Inter-Tropical Convergence Zone (ITCZ), Sub-tropical Anticyclones, Tropical Cyclones, Congo air mass and Global tele-connections.

1.6.1 Inter-tropical Convergence Zone

The Inter-Tropical Convergence Zone (ITCZ) is the main synoptic scale system that controls the intensity and migration of the seasonal rainfall over the Eastern Africa region. It marks the convergence zone of hemispheric monsoonal wind systems. It is a boundary of confluence of hemispheric winds near the surface as a result of inter-hemispheric monsoon wind system over the region. Due the complex effects of topographical diversity and low level synoptic circulation, the convergence is difficult to locate at low levels over Eastern Africa.

1.6.2 Sub-tropical Anticyclones

Sub-tropical anticyclones are synoptic scale quasi-permanent high pressure cells. They are characterized by anticyclonic circulation which gives rise to subsidence and low level horizontal velocity divergence of air masses. The four major anticyclones, which influence the flow of winds over the region are; the St. Helena high pressure system to the south west of Atlantic ocean, the Mascarene high pressure system to south east Indian ocean, the Arabian high in the middle east and Azores high pressure system which control the position and the movement of ITCZ as well as the Congo Air mass regime over the central and south-east of Africa.

1.6 .3 Tropical Cyclones

The tropical cyclones that influence weather in eastern and southern Africa form in the west Indian ocean equator-ward of 20° latitude north of the equator, they form in the northern spring and late fall and move northwards into the Arabian sea. The cyclones that have significant influence in eastern Africa are those that forming the south-west Indian ocean from December to April.

1.6.4 Global Scale and Regional Scale Systems

El Niño / Southern oscillation (ENSO), global sea surface temperatures (SSTs), Quasi-biennial Oscillation (QBO), Indian Ocean Dipole, (IOD), Intraseasonal waves (i.e Madden Julian Oscillation MJO) are the major climatic systems that affect rainfall over Rwanda through tele-connections.

1.6.5 Local Systems

Despite being located in the tropical belt, Rwanda experiences a temperate climate as a result of its high elevation. The North-western part is mountainous and volcanic with elevations over 2000m. Elevations reduce towards the central plateau (1500 - 2000m) of Rwanda and then again in the eastern plateau towards the border with Tanzania (less than 1500m). The highlands of these regions enhance convective development through orographic lifting and low convection over the East due to the lack of orographic lifting.

CHAPTER TWO

2.0 LITERATURE REVIEW

In East Africa, spatial analysis of satellite derived OLR revealed an active convection over the western parts of the region(Ogallo and Nyakwanda,1994). Salby and Hendon (1994) investigated the use of OLR in studying interseasonal variability. The study of Otieno and Anyamba (1994) used outgoing longwave radiation to establish its relationship with rainfall and reveaved that decresed outgoing longwave radiation was associated with enhanced rainfall over East Africa. Mutai (2000) found a strong correlation existing between OLR anomalies and standardized rainfall during the short rains (October to December) and a week correlation during the long rains season (March to May).

The linear relationship justified the use of outging longwave radiation to quantify the estimate of precipitation or its use as proxy to rainfall especially during October to December season. Omeny (2006) in his study of the East African rainfall variability associated with the Madden-Julian Oscillation, revealed a strong association between East African rainfall and MJO to the west of the region especially around the lake victoria basin.

He also found that strong convective development to the west associated with westerly and easterly winds configuration at 700hpa and 200hpa favors the relationship between rainfall and the convectively driven MJO.

Okoola (1996) used OLR in locating the position of inter-tropical convergence zone (ITCZ) over Equatorial Eastern Africa by delineating zones of convection. Outgoing Longwave Radiation corresponds to cloud top temperature and is indicative of concetive development caused by large-scale circulation systems that exist in low-level convergence and upper level divergence (Anyamba,1990).

In the tropics where the fluctautions in land surface temperatures are small. Outgoing Longwave Radiation reflects variations in cloudness or rainfall and can be used as proxy of convection capture convectively driven MJO along the equator (Madden and Julia (1994).

In East Africa the choice of 700hpa level is based on the fact that near the near the surface, the surface roughness due to terrain, vegetation etc influences the free flow of large-scale wind (Mukabana, 19992) resulting to reduced maximum convective activity. Maximum convective activity over East Africa is associated to westerly wind intensity at 700hpa level and easterly winds in the upper level (Okoola, 1996).

CHAPTER TWO

2.0 LITERATURE REVIEW

In East Africa, spatial analysis of satellite derived OLR revealed an active convection over the western parts of the region(Ogallo and Nyakwanda,1994). Salby and Hendon (1994) investigated the use of OLR in studying interseasonal variability. The study of Otieno and Anyamba (1994) used outgoing longwave radiation to establish its relationship with rainfall and reveaved that decresed outgoing longwave radiation was associated with enhanced rainfall over East Africa. Mutai (2000) found a strong correlation existing between OLR anomalies and standardized rainfall during the short rains (October to December) and a week correlation during the long rains season (March to May).

The linear relationship justified the use of outging longwave radiation to quantify the estimate of precipitation or its use as proxy to rainfall especially during October to December season. Omeny (2006) in his study of the East African rainfall variability associated with the Madden-Julian Oscillation, revealed a strong association between East African rainfall and MJO to the west of the region especially around the lake victoria basin.

Omeny also found that strong convective development to the west associated with westerly and easterly winds configuration at 700hpa and 200hpa favors the relationship between rainfall and the convectively driven MJO.

Okoola (1996) used OLR in locating the position of inter-tropical convergence zone (ITCZ) over Equatorial Eastern Africa by delineating zones of convection. Outgoing Longwave Radiation corresponds to cloud top temperature and is indicative of concetive development caused by large-scale circulation systems that exist in low-level convergence and upper level divergence (Anyamba,1990).

In the tropics where the fluctautions in land surface temperatures are small. Outgoing Longwave Radiation reflects variations in cloudness or rainfall and can be used as proxy of convection capture convectively driven MJO along the equator (Madden and Julia (1994).

In East Africa the choice of 700hpa level is based on the fact that near the near the surface, the surface roughness due to terrain, vegetation etc influences the free flow of large-scale wind (Mukabana, 19992) resulting to reduced maximum convective activity. Maximum convective activity over East Africa is associated to westerly wind intensity at 700hpa level and easterly winds in the upper level (Okoola, 1996).

CHAPTER THREE

3.0 Theoretical Framework

The Madden Julian Oscillation (MJO) is an intraseasonal fluctuation or "wave" occurring in the global tropics and moves eastwards with an identifiable wave pattern round the global tropics. The MJO is responsible for the majority of weather variability in these regions and results in variations in several important atmospheric and oceanic parameters which include both lower- and upper-level wind speed and direction, cloudiness, rainfall, sea surface temperature (SST), and ocean surface evaporation. The MJO is a naturally occurring component of our coupled ocean-atmosphere system and the typical length of the MJO cycle or wave is approximately 30-60 days (Madden and Julian, 1971, 1972; Madden and Julian, 1994; Zhang, 2005).

The MJO is characterized by eastward propagation of regions of enhanced and suppressed tropical rainfall, primarily over the Indian and Pacific Oceans. The anomalous rainfall is often first evident over the Indian Ocean, and remains apparent as it propagates eastward over the very warm waters of the western and central tropical Pacific. Over the cooler ocean waters of the eastern Pacific, the pattern of tropical rainfall generally becomes nondescript, but often reappears over the tropical Atlantic and Africa. Along with these variations in tropical rainfall, there are distinct patterns of lower- and upper-level atmospheric circulation anomalies in the tropics and subtropics. These features extend around the globe and are not confined to the eastern hemisphere. Thus, they provide imortant information regarding the regions of ascending and descending motion associated with particular phases of the oscillation.

Figure 2 illustrates an equatorial vertical cross section of the MJO showing the changes in cloudiness, rainfall, wind speed and direction, and SST as the MJO propagates eastward around the global tropics (Adapted from Madden and Julian, 1971;1972).
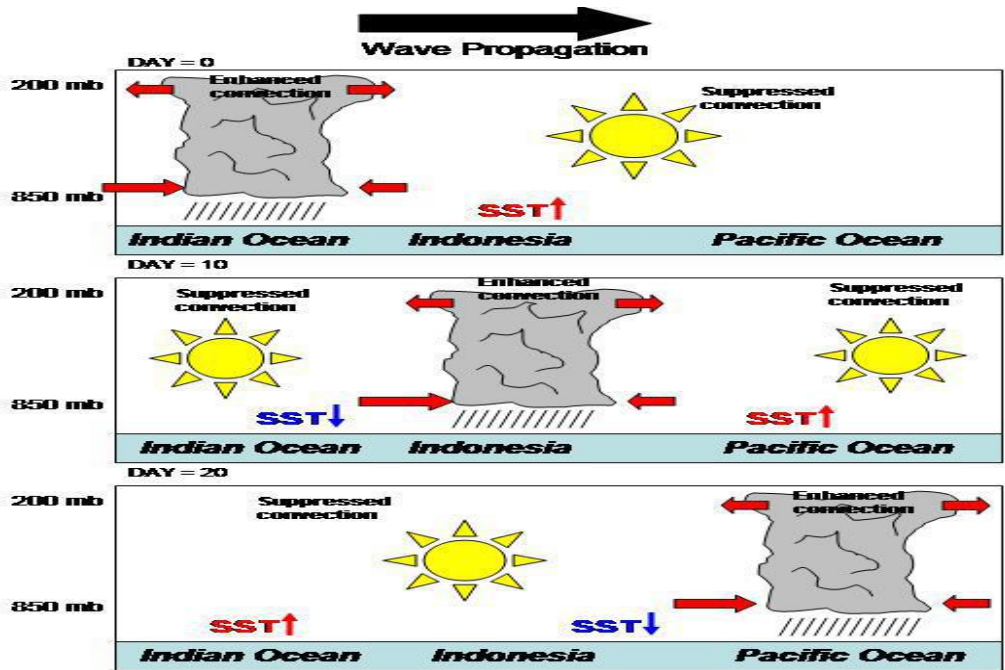
Figure 2: Equatorial vertical cross section of the MJO as it propagates from the Indian Ocean to the western Pacific. Red arrows indicate direction of wind and red (blue) SST labels indicate positive (negative) SST anomalies respectively. (Figure adapted from Madden and Julian, 1971; 1972.)

By combining many MJO events together into composites, we obtain an idealized representation of the three dimensional structure of the MJO (Figure 3).
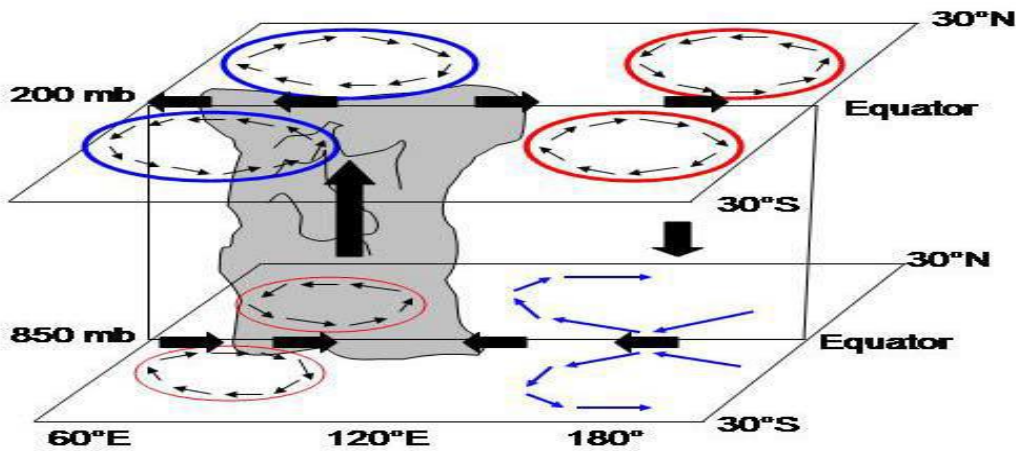
Figure 3: Schematic of the vertical three-dimensional structure of an established MJO. Blue (red) ovals indicate anticyclonic (cyclonic) circulations. Black arrows indicate wind direction and rising (sinking) motion (Adapted from Rui and Wang, 1990).

10

When convection is active in the Indian Ocean and Indonesia, anomalous easterlies (westerlies) exit the area of enhanced convection in the upper levels of the atmosphere and associated with anti-cyclonic gyres along and behind the area of enhanced convection. Conversely, cyclonic gyres exist behind areas of suppressed convection in both hemispheres. At low levels, anomalous easterlies (westerlies) are evident ahead (behind) the area of enhanced convection. The low level gyres are generally weaker than those at upper levels. As the dipole propagates toward the central Pacific, the lower and upper level circulation anomalies become less recognizable and coherent but remain an important component in redistributing mass around the global tropics.

There is strong year-to-year variability in MJO activity, with periods of strong activity followed by long periods in which the oscillation is weak or absent (Hendon et al. 1999; Zhang, 2005). There is evidence that the interannual variability of the MJO is partly linked to the ENSO cycle. Strong MJO activity is often observed during weak La Niña years or during ENSO-neutral years, while weak or absent MJO activity is typically associated with strong El Niño episodes. Figure 4 illustrates MJO activity for three different September through June time periods via time longitude plots of velocity potential (a measure of thedivergence of air in the upper atmosphere).
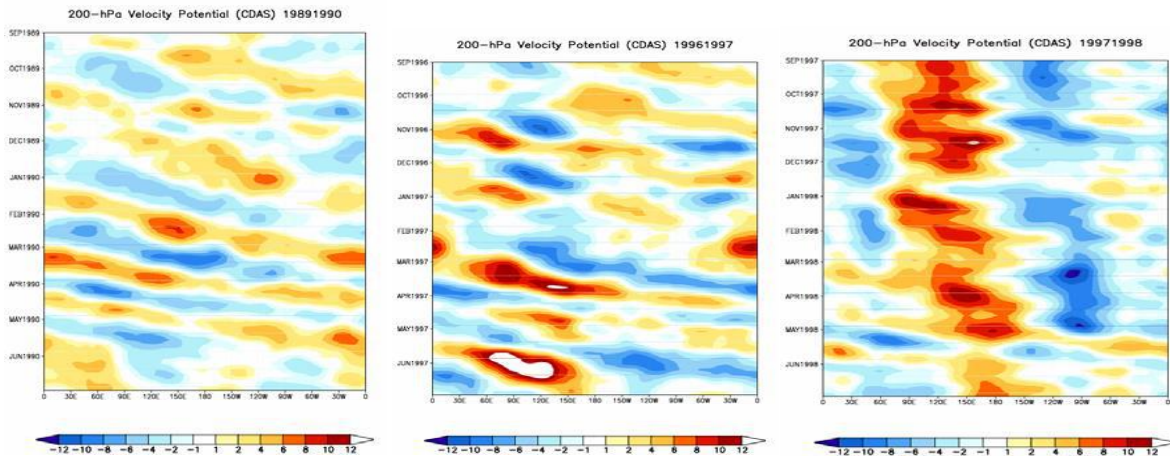
Figure 4: Time longitude plots of 200-hPa velocity potential for the June through September time period for (a) 1989-1990 (La Niña conditions), (b) 1996-1997 (ENSO neutral conditions), and (c) 1997-1998 (El Niño conditions).

The first figure shows regular but generally weak to moderate MJO activity during 1989-1990 while during 1996-1997 there are periods of strong MJO episodes but with less regularity. The final panel shows virtually no MJO activity as little eastward propagation is evident with the most dominant feature of variability being the interannual ENSO (El Nino) signal.

Well established, coherent MJO activity results in key atmospheric anomalies that can potentially have wide ranging impacts. In areas of upper level divergence (negative velocity potential) enhanced rainfall can occur. Favored regions over land include Northeast Brazil, Southeast Africa, and Indonesia during boreal winter and Central America/Mexico and Southeast Asia during boreal summer (Knutson and Weickmann, 1987; Rui and Wang, 1990; Kayano and Kousky, 1999).

The MJO can substantially modulate the intensity of monsoon systems around the globe. The Australian (boreal winter; October-March), Asian (boreal summer; June-September), South American (boreal winter, October-March) and North American (boreal summer; May-October) monsoons can all be influenced by the MJO. The enhanced rainfall phase of the MJO can affect both the timing of monsoon onset and the intensity of the monsoon. Moreover, the suppressed phase of the MJO can prematurely end a monsoon and also initiate breaks during already existing monsoons.

The MJO also enhances (suppresses) the intensity and extent of both the mean South Atlantic Convergence Zone (SACZ; Brazilian coast) and South Pacific Convergence Zone (SPCZ; east of Australia) (Matthews et al. 1996; Carvalho et al. 2004).

There is evidence that the MJO influences the ENSO cycle. It does not cause El Niño, but can contribute to the speed of development, and perhaps the overall intensity of El Niño episodes (Kessler and Kleeman,2000; Zhang and Gottschalck, 2002).

The MJO is known to modulate tropical cyclone activity in the Indian Ocean, Pacific Ocean, Gulf of Mexico, and Atlantic Ocean (Maloney and Hartmann, 2000a; Maloney and Hartmann, 2000b; Higgins and Shi, 2001). For example, although tropical cyclones occur throughout the Northern Hemisphere warm season (typically May-November) in both the Pacific and the Atlantic basins, in any given year there are periods of enhanced / suppressed activity within the season. The MJO modulates this activity (particularly for the strongest storms) by providing a large-scale environment that is favorable (unfavorable) for ndevelopment. For example, westerly wind anomalies at the surface in and just behind the area of enhanced convection of the MJO may generate cyclonic (anticyclonic) rotation north (south) of the equator respectively.

At the same time, in the upper levels, anticyclonic (cyclonic) rotation develops along and just behind the area of convection (Figure 2) resulting in a means to reduce vertical wind shear and increase upper-level divergence – both of which are favorable for tropical cyclone development and intensification. The strongest tropical cyclones tend to develop when the MJO favors enhanced precipitation. As the MJO progresses eastward, the favored region for tropical cyclone activity also shifts eastward from the Indian Ocean to the Pacific Ocean and eventually to the Atlantic Ocean.While this relationship appears robust, we caution that the MJO is one of many factors that contribute to the development of tropical cyclones. For example, it is well known that SSTs must be sufficiently warm and vertical wind shear must be sufficiently weak for tropical disturbances to form and persist.

Enhanced tropical rainfall in the western and central Pacific can contribute to extreme rainfall events in western North America (Higgins et al. 2000). The typical scenario linking the pattern of tropical rainfall associated with the MJO to extreme precipitation events in the Pacific Northwest features a progressive (i.e.eastward moving) circulation pattern in the tropics and a retrograding (i.e. westward moving) circulationpattern in the high latitudes of the North Pacific.

CHAPTER FOUR

4.0 DATA AND METHODOLOGY

4.1 Data

Daily rainfall data from 1979 to 2013 for five stations over Rwanda were collected from the Rwanda Meteorology Agency headquarters located in Kigali. The MJO indices are available from June 1974 to present. These indices were freely available on-line from (http://cawcr.gov.au/staff/mwheeler/maproom/RMM/RMM1RMM2.74toRealtime.txt). The choice of MJO indices from 1979 is based on the continuity of data as opposed to data from 1794, which has some missing data in 1978. The choice of data from 1979 was choosen to reflect the MJO indices.

4.1.1 Data Quality Control

Data quality control involved estimation of missing data and homogeneity test. Several methods are use in estimation of missing data. In this sturdy, missing data were estimated using longterm mean method that involved replacing missing record with the average value for given stations. The quality of the estimated data was examined using cumulative mass curve. In this study single mass curve was used to indicate homogeneity for stations that were found to be correlated.

The Figure 5 shows the single mass curves for five stations used in this study.

14
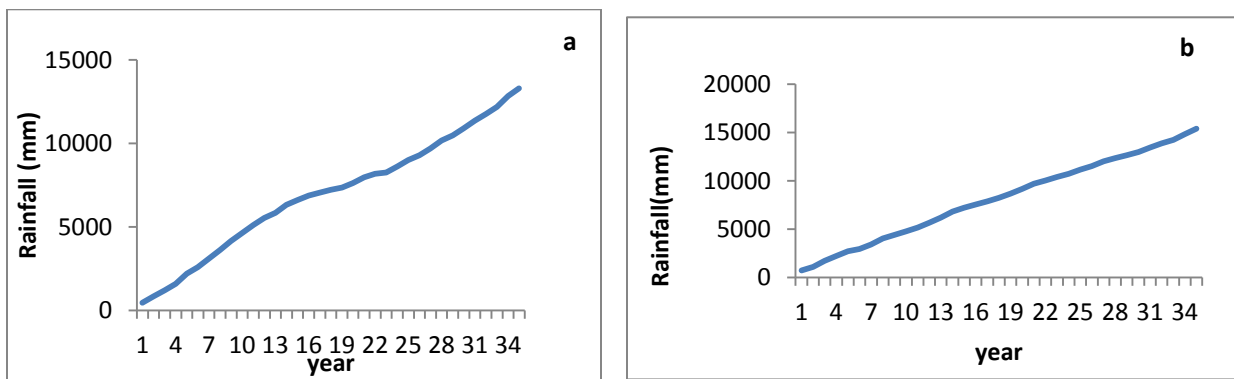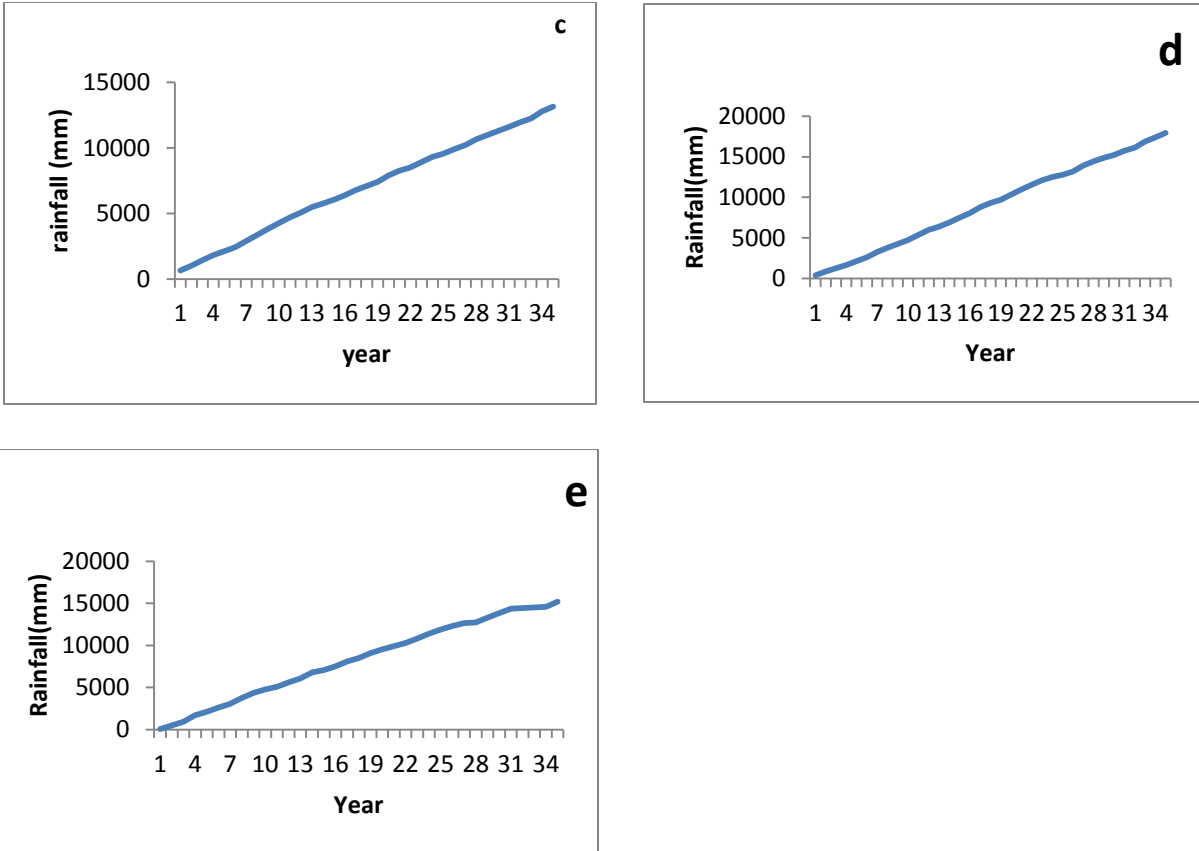
Figure 5: Single mass curves of daily rainfall during March-May season at (a) Kamembe, (b) Gikongoro, (c) Kigali, (d) Byumba and (e) Kibungo stations.

4.2 Methodology

The methods used include temporal and spatial analysis, frequency analysis, and composite analysis and correlation analyses.

4.2.1 Temporal and Spatial Analysis

In this study, the temporal and spatial analyses methods were used to achieve the first specific objective which was to determine the temporal and spatial variability of rainfall based on daily rainfall over Rwanda during the March-May season. Temporal variability of rainfall was investigated using a time series analysis. Thus the daily rainfall data were subjected to time series analysis. Plotting of time series involved rainfall data against time. Examination of the trend in a time series is significant since it will show where time series is stationary or non-stationary. Spatial variability of rainfall was analyzed using Suffer software that will provide

15

spatial map. Plotting involves latitude longitude against rainfall data, thus this method enable us to know how rainfall varies from one place to another.

4.2.2 Frequency Analysis

The frequency analysis method was used to achieve the second specific objective which involved determining the frequence of occurence of wet and dry spells during March-May season over Rwanda. The rainfall greater than 1mm is considered as a wet event while rainfall less than 1mm is considered as dry event.

4.2.3 Composite and Correlation Analyses

Composite and Correlation analyses methods were used to achieve the third specific objective of the study, which was to determine the progression of the Madden-Julian Oscillation during the March-May season on a daily basis. The method involves identifying and averaging one or more categories of fields of a variable selected according to their association with key conditions (Folland et al, 1983). It involves summarizing meteorological element,where the composite is the mean of the element averaged over a number of cases sampled out according to a certain similarity. Many authors including Ininda (1998) and Okoola (1999) have used composite analysis method to perform composite for wet years and dry years separetely. Composites are usefull for indicating pronounced and common features and patterns in variables.

The correlation analysis measures the degree of association between MJO indices with daily rainfall. The correlation coefficient 'r' was measured to show the strength of the relationship between the variables. For N pairs of observations, x and y, the correlation coefficient (r) is obtained by using the following expression below:

$$r = \frac{\sum_{i=1}^{n}(X_i - \bar{X})(Y_i - \bar{Y})}{\sqrt{\sum_{i=1}^{n}(X_i - \bar{X})^2}\sqrt{\sum_{i=1}^{n}(Y_i - \bar{Y})^2}}$$

Equation (1):

In Equation (1):

  r is the correlation coefficient and its value ranges between -1 and +1,

X_i is the ith value of the variable X,

Y_i is the ith value of the variable Y,

$\bar{X}$ is the mean of variable X and

$\bar{Y}$ is the mean of variable Y

CHAPTER FIVE

5.0 RESULTS AND DISCUSSION

5.1 Temporal and Spatial analysis

Temporal and spatial variability based on daily rainfall over Rwanda during March-May season has been performed using temporal and spatial analysis for five stations each representing a homogeneous climatezone over the country. Temporal variability of the daily rainfall data were subjected to time series analysis.

Figure 6 indicates the temporal variability of rainfall during MAM season. Figure 6a shows that the rainfall peaks during the first week of March and decreases in the third week of May.

The high frequency of rain days occurred between the third weak of March to the second week of May. The convective activity over this region may be attributed to the strong westerly wind which inject moisture from congo basin. The highlands of these regions also enhance convective development through orographic lifting.

Figure 6b shows that the rainfall peaks during the third week of March and decreases in the third week of May. The high frequency of rain days occurred between the third week of March and the second week of March. The convective activity over this region may be attributed to the strong westerly wind which inject moisture from congo air mass. The highlands of these regions also enhance convective development through orographic lifting and to the fact that this region is located near the Nyungwe national park.

Figure 6c shows that the rainfall peaks during the second week of March and decreases in the third week of May. The high frequency of rain days occurred within the month of April and the second week of March. The convective activity over this region may be attributed to easterly wind which inject moisture fron lake Victoria and indian ocean and the highlands of thise region also enhance convective development through orographic lifting.

Figure 6d shows that the rainfall peaks during the second week of March and decreases in the third week of May. The high frequency of rain days occur between the third week of March and the third week of March. The convective activity over this region may be attributed to the strong

westerly wind which inject moisture from congo basin. The highlands of these regions (volcanic region) also enhance convective development through orographic lifting.

Figure 6e shows that the rainfall peaks during the second week of March and decreases in the third week of May. The high frequency of rain days occur within the month of April and the first two weeks of March. Low concective development to the Eastern part of the country may be attributed to Easterly wind which inject moisture fron lake Victoria and indian ocean and to the lack of orographic lifting
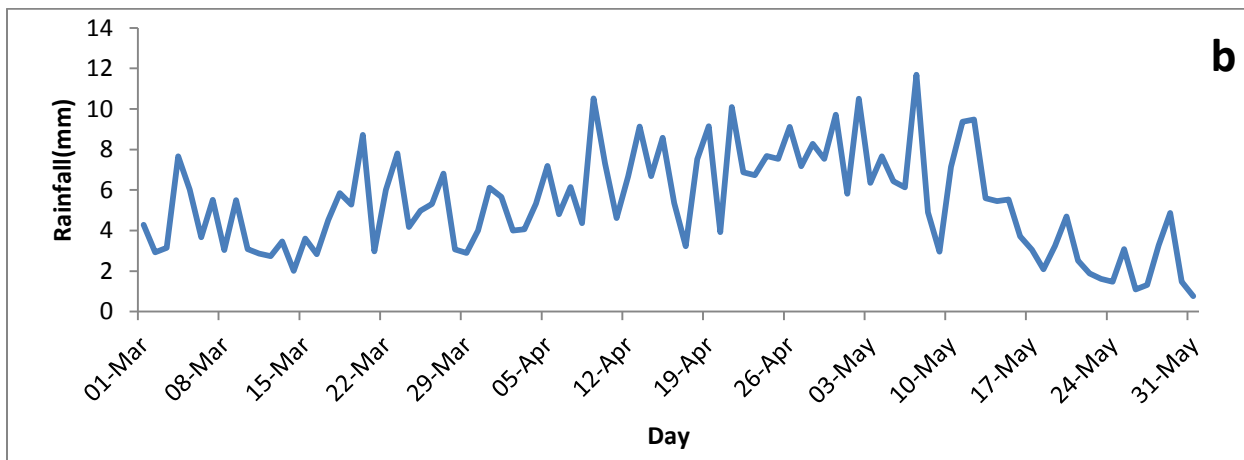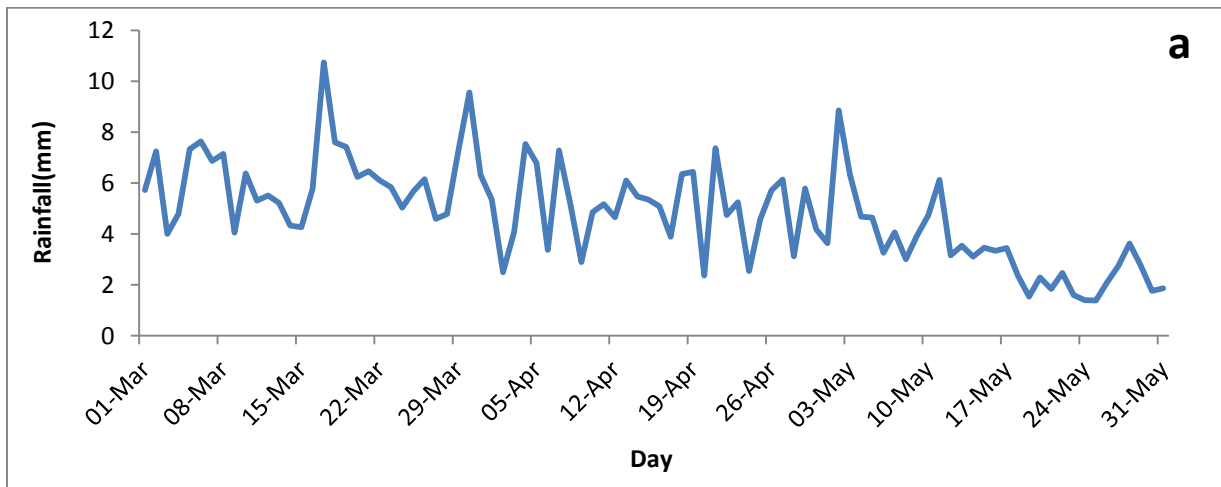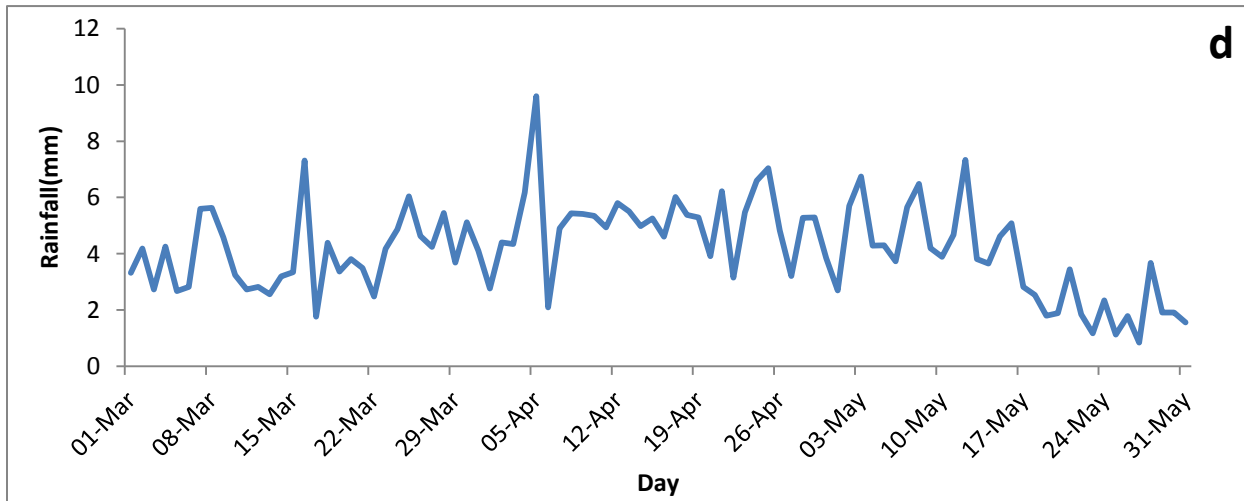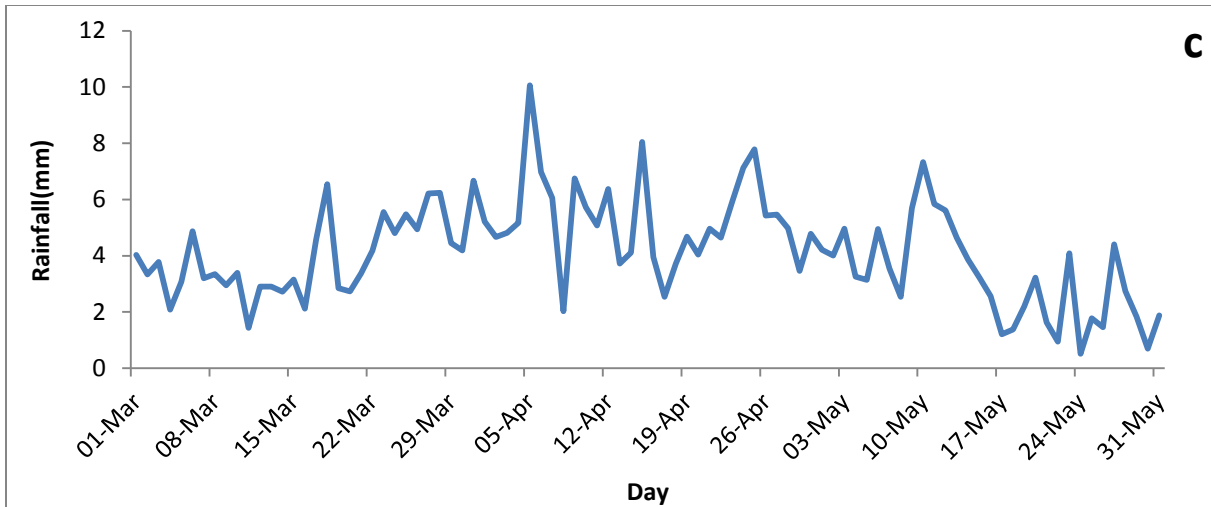
Figure 6: Temporal variability of daily mean rainfall (mm) between 1979 and 2013 from 1 March and 31 May at (a) Kamembe, (b) Gikongoro, (c) Kigali, (d) Byumba and (e) Kibungo stations.

20

Spatial variability of rainfall was analyzed using suffer and Plotting involves latitude longitude against rainfall data. Figure 7 shows the Spatial variability of rainfall over Rwanda during MAM season on day by day basis. The figure shows that the rainfall increases westward; the highest rainfall is in the south of the country and low rainfall in the East of the country. High rainfall over this region may be attributed to the strong westerly wind which inject moisture from congo basin. The highlands of these regions also enhance convective rainfall development through orographic lifting. The low rainfall over the eastern part of the country may be attributed to the easterly wind which injects moisture fron lake Victoria and Indian Ocean and to the lack of orographic lifting.
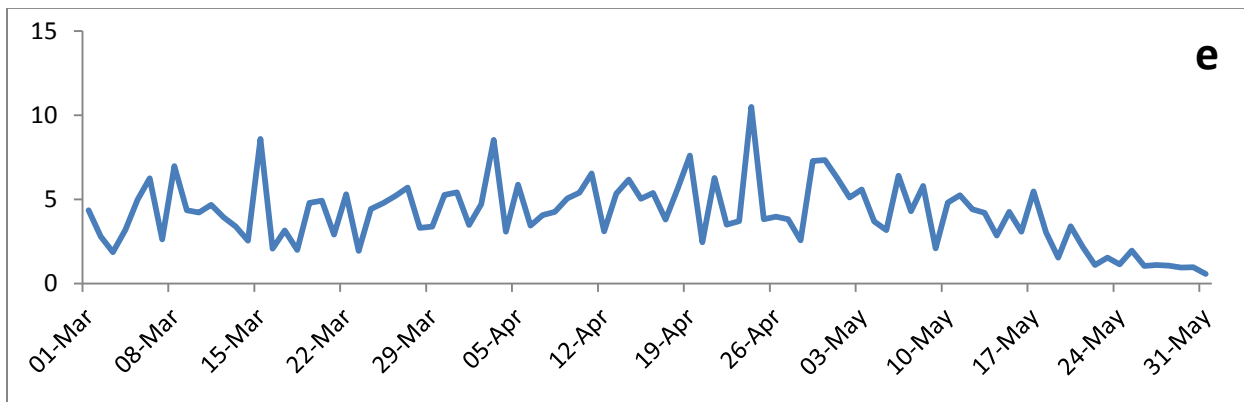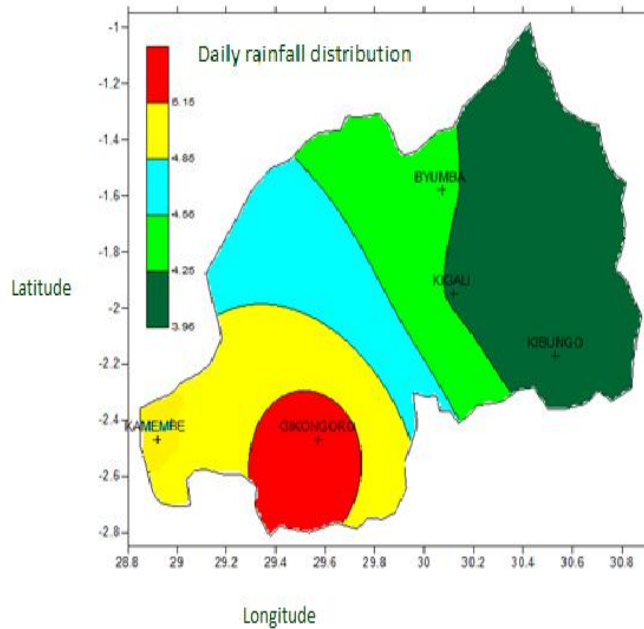

Figure 7: Spatial variability of rainfall over Rwanda during MAM season on day by day basis.

5.2 Wet and Dry Spells

The frequencies of wet and dry spells over Rwanda based on daily rainfall during MAM season, have been assessed, the wet spell is determined for rainfall greater than 1mm and dry spell as rainfall less than 1 mm.

The considerable numbers of wet spells during the MAM season are located between the third week of March to the second week of May while the considerable numbers of dry spells during the same season are located within the last two weeks of May. Figure 8 indicates the wet and dry Spells over Rwanda.

 Figure 8a shows that the considerable number of wet spells during the MAM season over Kamembe occurred between the third week of March to the second week of May and the period of the season with high number of wet spells being the month of April with a peak on the 4th of April having a frequency of 30 wet events.

 Figure 8b shows that the considerable number of wet spells during the MAM season over Gikongoro occurred between the first week of April to the second week of May and the period of the season with high number of wet spells being the month of April with a peak on the 27th of March, having a frequency of 28 wet events.

Figure 8c shows that the considerable number of wet spells during the MAM season over Kigali occurred between the third week of March to the second week of May and the period of the season with high number of wet spells being the month of April with a peak on the 16th April having a frequency of 24 wet events.

Figure 8d shows that the considerable number of wet spells during the MAM season over Byumba occurred between the third week of March to the second week of May and the period of the season with high number of wet spells being the month of April with a peak on the 1st May having a frequency of 34 wet events.

 Figure 8e shows that the considerable number of wet spells during the MAM season over Kibungo occurred between the third week of March to the second week of May and the period

of the season with high number of wet spells being the month of April to the second week of May with a peak on the 30th May having a frequency of 30 wet events.

.
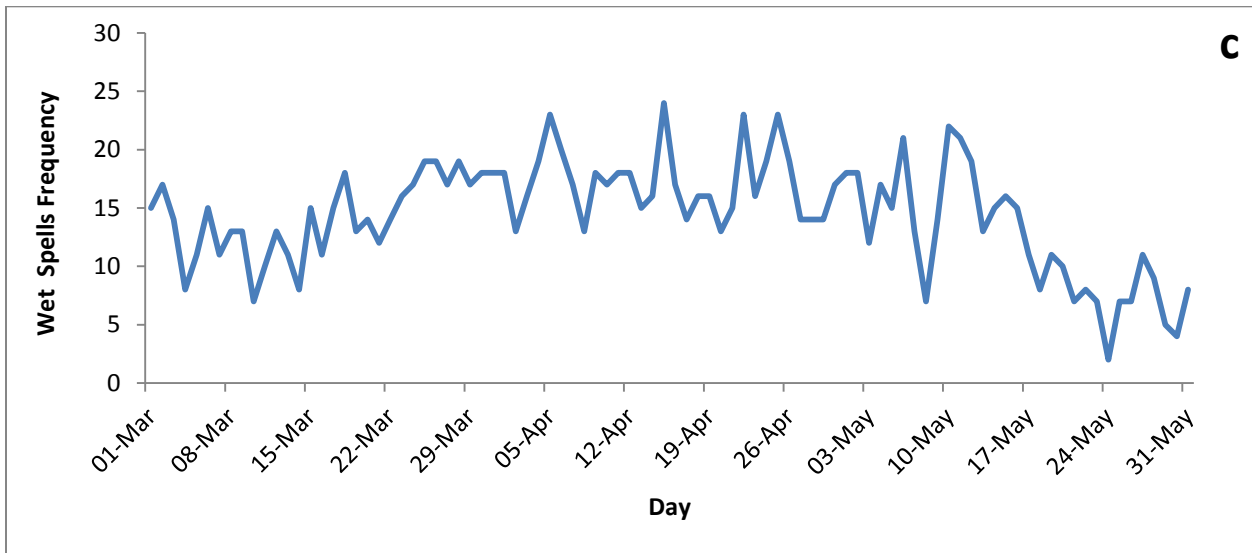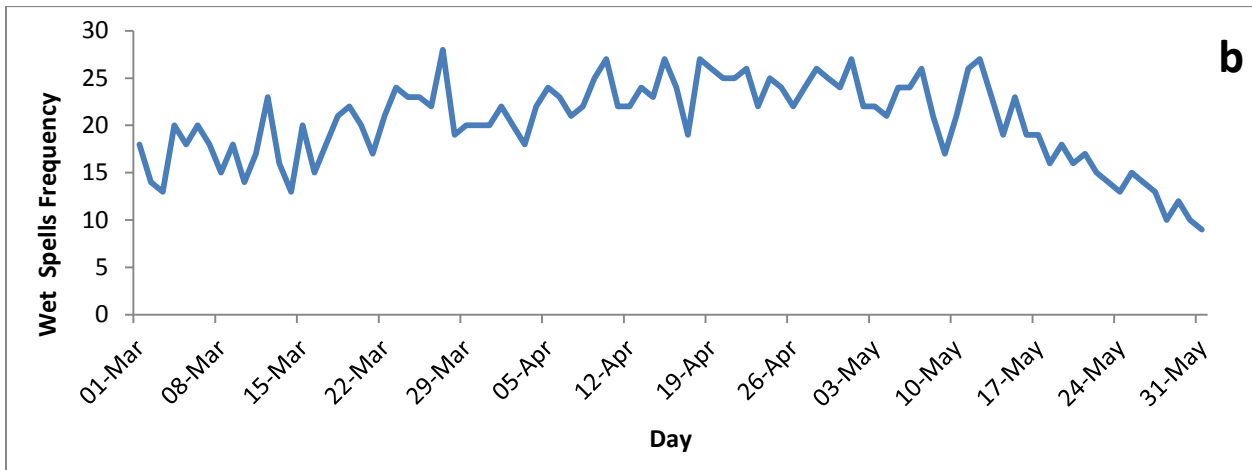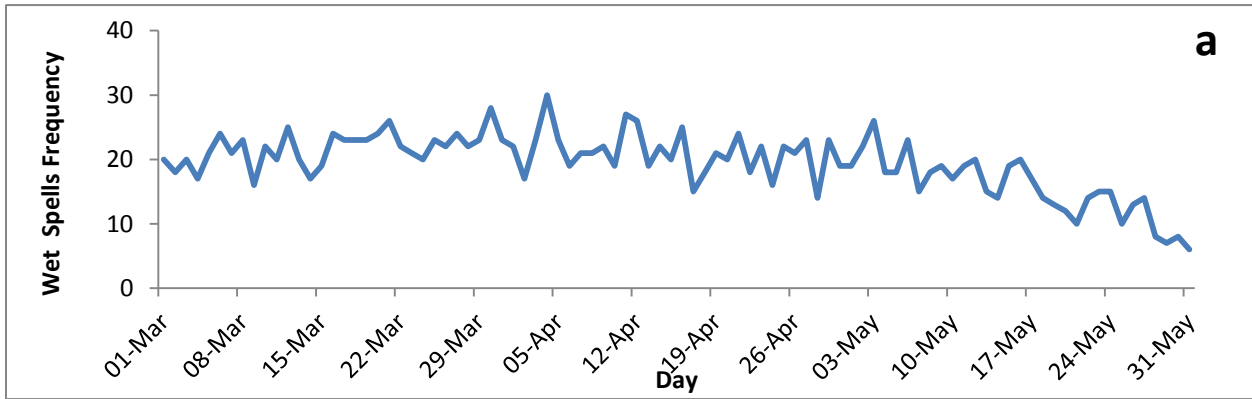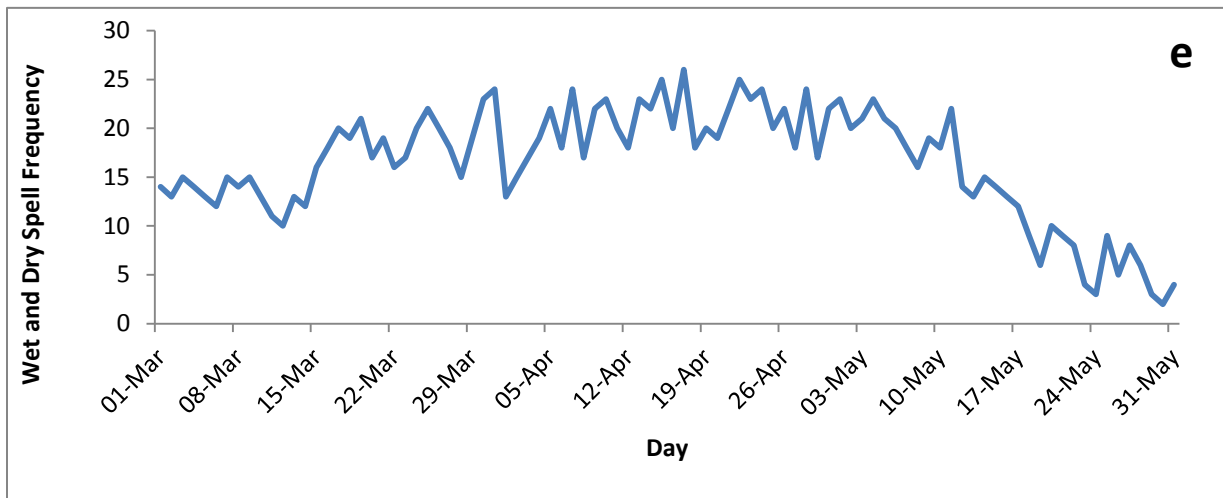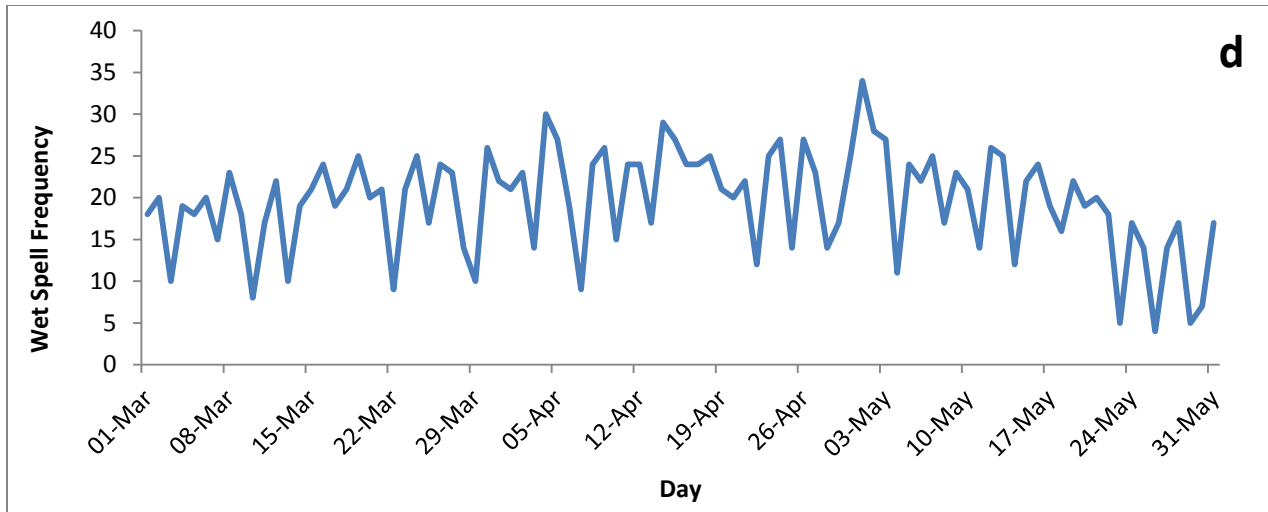
Figure 8: Wet Spells during the MAM season between 1979 and 2013 at (a) Kamembe, (b) Gikongoro, (c) Kigali,(d) Byumba and (e) Kibungo stations.

Figure 9 indicates the Dry Spells over Rwanda.

Figure 9a shows that the considerable number of dry spells during the MAM season over Kamembe occure within the the last two weeks of May with a peak on the 23rd of May with a frequency of 28 dry events.

Figure 9b shows that the considerable number of dry spells during the MAM season over Gikongoro occurred within the the last two weeks of May with a peak on the 31st of May with a frequency of 28 dry events.

Figure 9c shows that dry spells during the MAM season over Kigali occure within the the last two weeks of May with a peak on the 24th of May with a frequency of 30 dry events.

Figure 9d shows that the dry spells during the MAM season over Byumba within the the last week of May with a peak on the 23rd of May with a frequency of 29 dry events.

Figure 9e shows that the considerable number of dry spells during the MAM season over Kibungo occurred within the the last two weeks of May with a peak on the 30th of May with a frequency of 33 dry events.
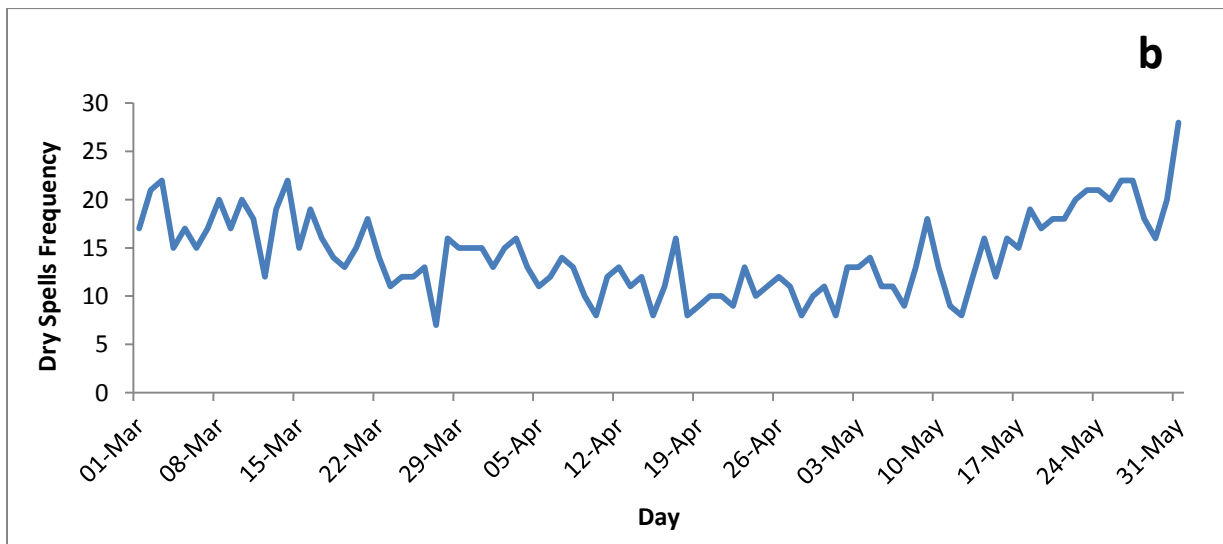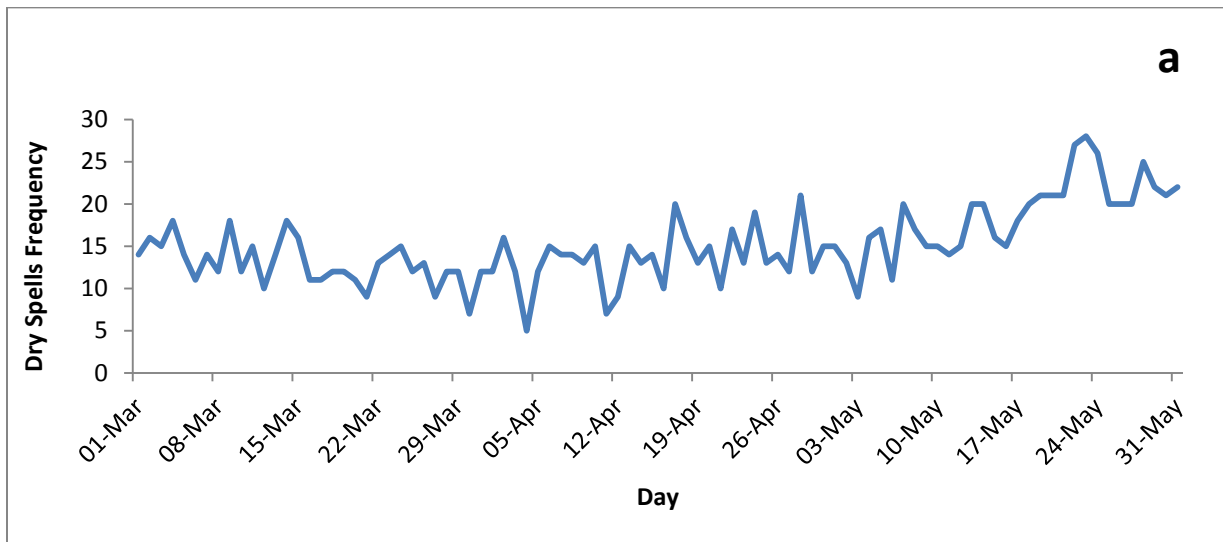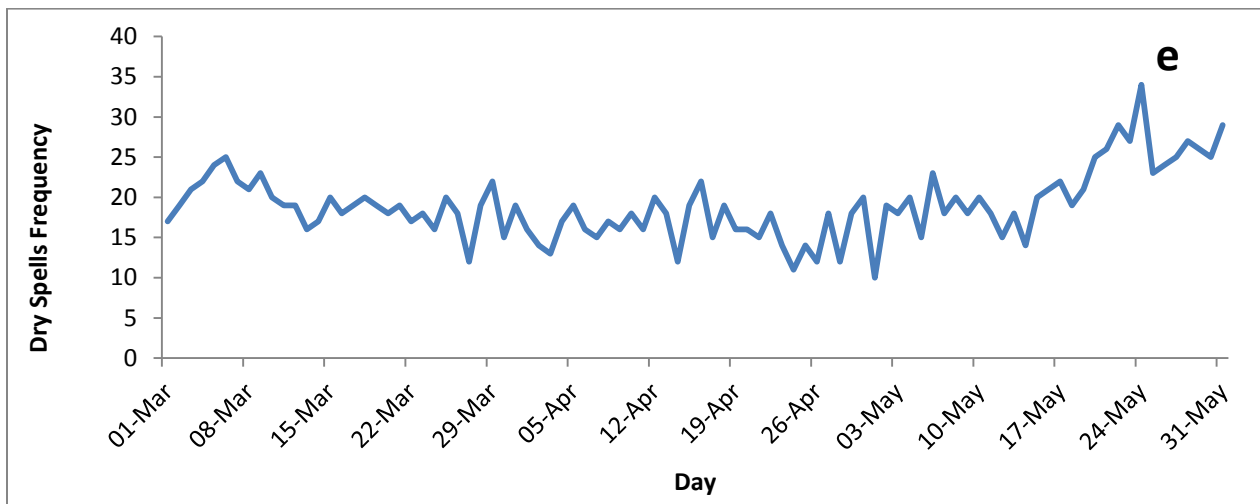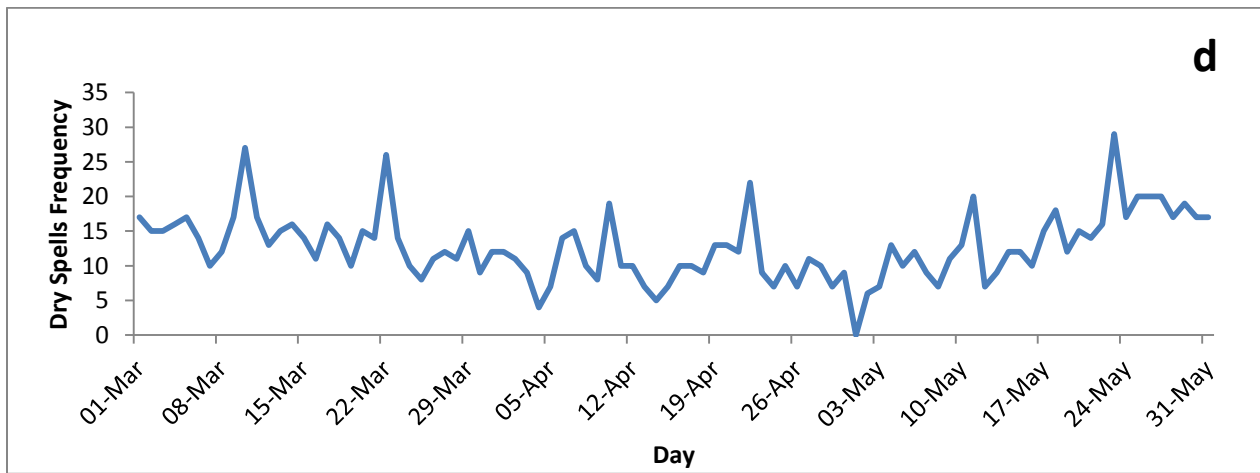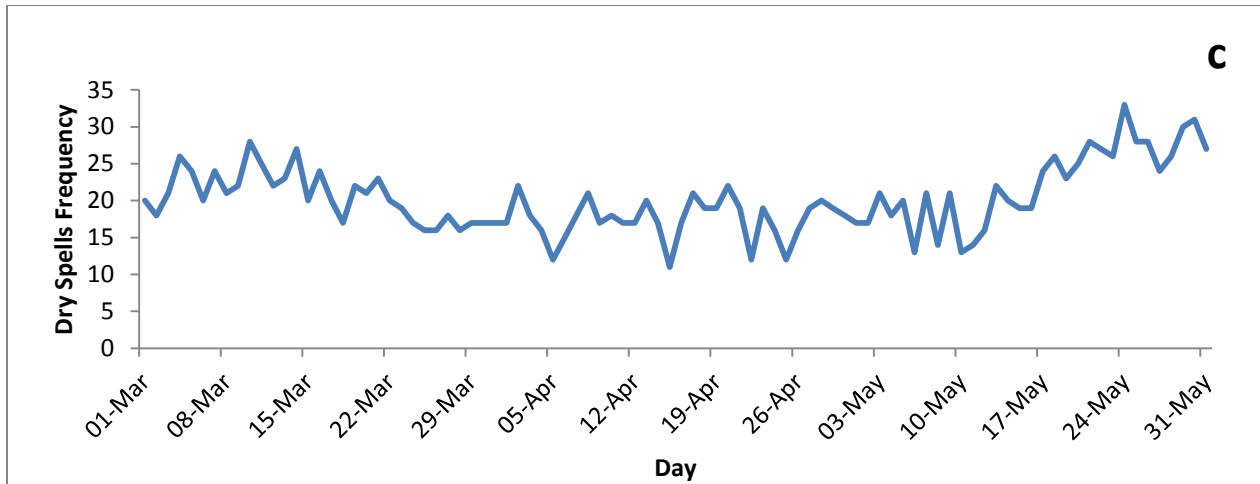
Figure 9: Dry Spells during the MAM season between 1979 and 2013 at (a) Kamembe, (b) Gikongoro, (c) Kigali,(d) Byumba and (e) Kibungo stations.

5.3 Composite Analysis

The composite of rainfall were computed by averaging rainfall day by day for the MAM season. Similarly the composite of MJO indices were computed by averaging wind indices and OLR indices for the season. The 5 days moving average were computed for both rainfall and MJO indices. The analysis of rainfall with wind indices indicate a positive pattern and an opposite pattern with OLR indices with rainfall lagging behand the MJO indices. The negative OLR reflect the low radiation emitted by the developed convective cloud while the positive OLR represent radiation emiteed in cloud in cloud free region.

The convective activity which may be associated with slightly high negative RRM2 value over the south, west and north west may be attributed to the westerly wind which inject moisture from Congo basin and the west fluctuation of the meridional arm of the ITCZ . the fluctuation of meridional arm of the ITCZ enhances convergence over the south, west and north west part of the country . The highlands of these regions also enhance convective development through orographic lifting. The deep convection over the south west may also be associated to the fact that this region is located near the Nyungwe national part. The concective development to the central and easter may be attributed to easterly wind which inject moisture fron lake Victoria and indian ocean, orographic lifting to the central and to the lack of orographic lifting to the eastern part of the country. Figure 10 shows the Daily variability of rainfall composite with MJO indices.

Figure 10a show the Daily variability of rainfall composite with MJO indices at Kamembe station. The positive pattern between the rainfall composite and the wind component was revealed while an opposite pattern between the rainfall composite and OLR component was indicated. This shows that an increase in the rainfall is associated with an incease of wind indices and a decrease in OLR indices. This may be attributed to the strong westerly wind which inject moisture from congo basin and the orographic lifting.

Figure 10b show the Daily variability of rainfall composite with MJO indices at Gikongoro station. An opposite pattern between the rainfall composite and OLR component was indicated

27

while a positive pattern between the rainfall composite and the wind component was revealed. This shows that a decrease in the rainfall is associated with increase in OLR indices.

and a decease of wind indices. This may be attributed to the strong westerly wind which inject moisture from congo basin , the orographic lifting and to fact that this area is located around Nyungwe National Park.

Figure 10c show the Daily variability of rainfall composite with MJO indices at Kigali station. The positive pattern between the rainfall composite and the wind component was revealed while an opposite pattern between the rainfall composite and OLR component was indicated. This shows that an increase in the rainfall is associated with an incease of wind indices and a decrease in OLR indices.This may be attributed to easterly wind which inject moisture fron lake Victoria and indian ocean and orographic lifting. to the central and to the lack of orographic lifting to the eastern part of the country.

Figure 10d show the Daily variability of rainfall composite with MJO indices at Byumba station. An opposite pattern between the rainfall composite and OLR component was indicated while a positive pattern between the rainfall composite and the wind component was revealed. This shows that a decrease in the rainfall is associated with increase in OLR indices.

and a decease of wind indices. This may be attributed to the strong westerly wind which inject moisture from congo basin , the orographic lifting and to fact that this area is located around volcanic region.

Figure 10e show the Daily variability of rainfall composite with MJO indices at Kibungo station. The positive pattern between the rainfall composite and the wind component was revealed while an opposite pattern between the rainfall composite and OLR component was indicated. This shows that an increase in the rainfall is associated with an incease of wind indices and a decrease in OLR indices.This may be attributed to easterly wind which inject moisture fron lake Victoria and indian ocean and to the lack of orographic lifting .
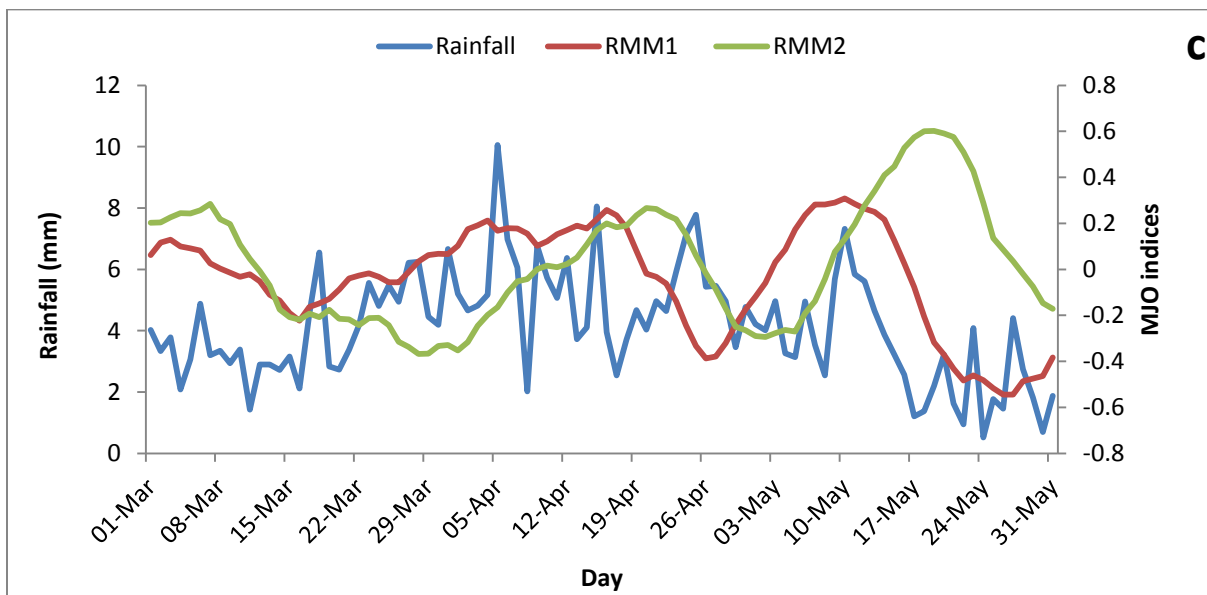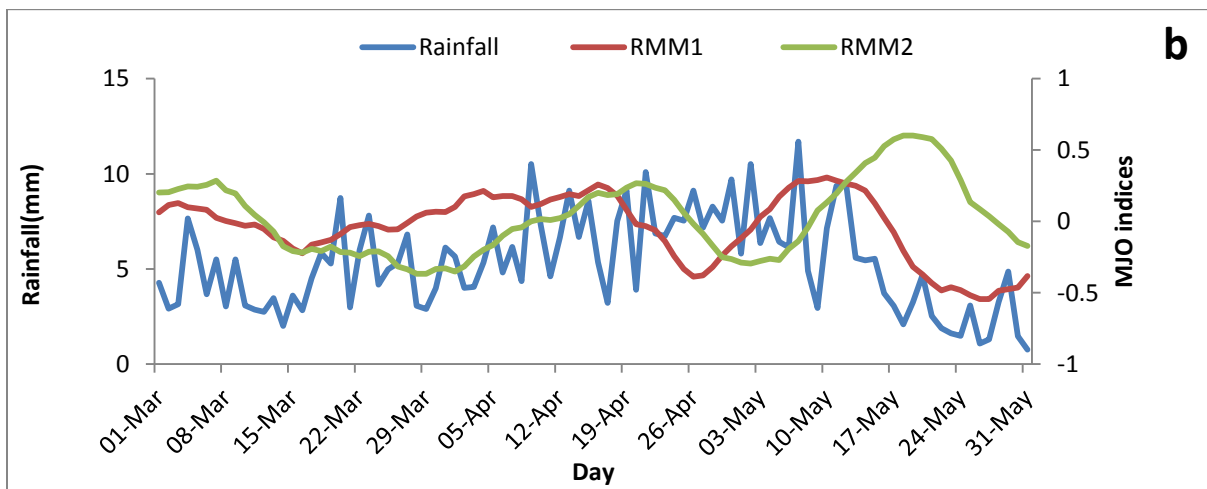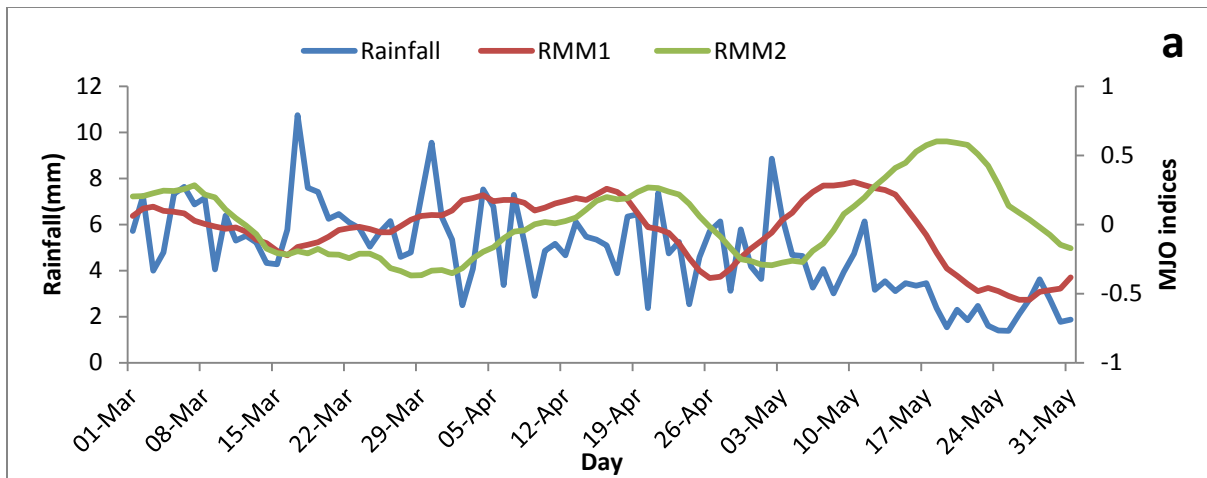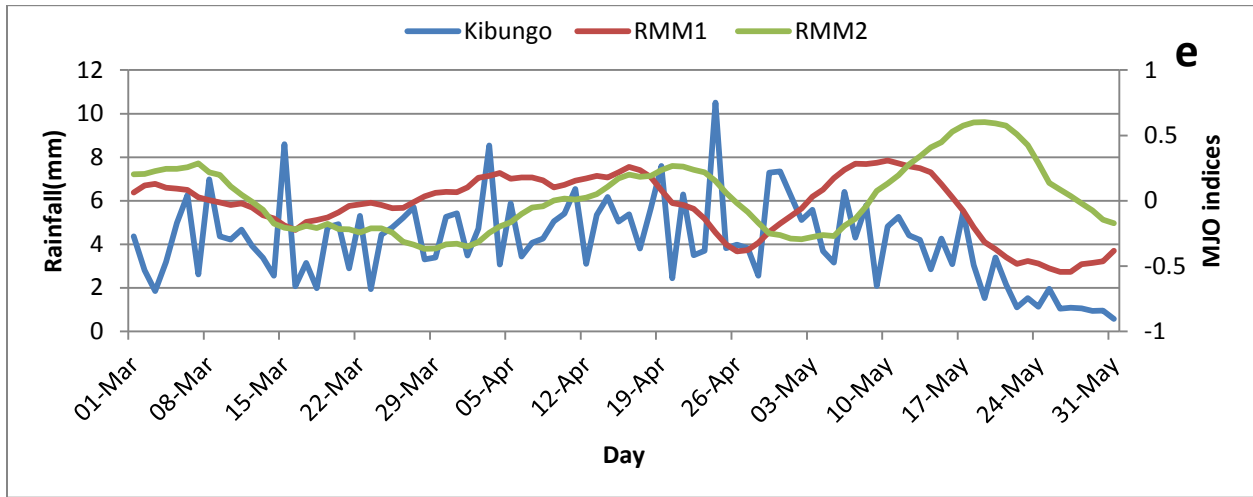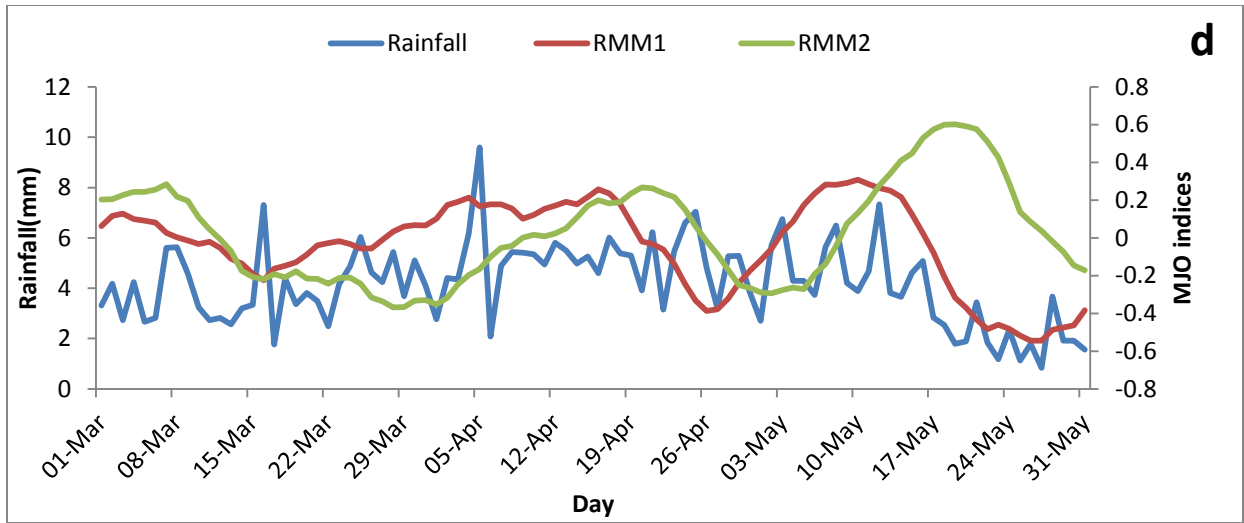
Figure 10: Daily variability of rainfall composite (blue) in mm, wind (red) and OLR (green) indices during MAM season averaged bewteen 1979 and 2013 at (a) Kamembe, (b) Gikongoro, (c) Kigali, (d) Byumba and (e) Kibungo.

Composite of rainfall anomalies with OLR anomalies indicate a well-established opposite pattern between the rainfall anomalies and the OLR component anomalies at lag five.

Figure 11 show the Daily variation of rainfall anomalies at lag five with RMM2 component over five stations.

Figure 11a show the Daily variation of rainfall anomalies at lag five with RMM2 component anomalies over Kamembe station. Figure 11a shows that the positive rainfall anomalies correspond to the negative OLR anamalies which reflect the low radiation emitted by the

developed convective cloud during the second week of March to the second week of April while the negative rainfall anomalies corespond to the positive OLRanomalies which reflect radiation emiteed in cloud free region during the fourth week of April to the fourth week of May.

Figure 11b show the Daily variation of rainfall anomalies at lag five with RMM2 component over Gikongoro station. Figure 11b shows that the positive rainfall anomalies correspond to the negative OLR anamalies which reflect the low radiation emitted by the developed convective cloud during the first week of March to the first week of April while the negative rainfall anomalies corespond to the positive OLR anomalies which reflect radiation emiteed in cloud free region during the fourth week of April to the fourth week of May.

Figure 11c shows the Daily variation of rainfall anomalies at lag five with OLR component anomalies over Kigali station. Figure 11c shows that the negative rainfall anomalies corespond to the positive OLRanomalies which reflect radiation emiteed in cloud free region during the fourth week of April to the fourth week of May while positive rainfall anomalies correspond to the negative OLR anamalies which reflect the low radiation emitted by the developed convective cloud during the first week of March to the first week of April.

Figure 11d show the Daily variation of rainfall anomalies at lag five with OLR component anomalies over Byumba station. Figure 11d shows that the positive rainfall anomalies correspond to the negative OLR anamalies which reflect the low radiation emitted by the developed convective cloud during the second week of March to the first week of April while the negative rainfall anomalies corespond to the positive OLRanomalies which reflect radiation emiteed in cloud free region during the third week of April to the fourth week of May.

Figure 11e show the Daily variation of rainfall anomalies at lag five with OLR component anomalies over Kibungo station. Figure 11e shows that the positive rainfall anomalies correspond to the negative OLR anamalies which reflect the low radiation emitted by the developed convective cloud during the first week of March to the second week of April while the negative rainfall anomalies corespond to the positive OLRanomalies which reflect radiation emiteed in cloud free region during the third week of April to the fourth week of May.
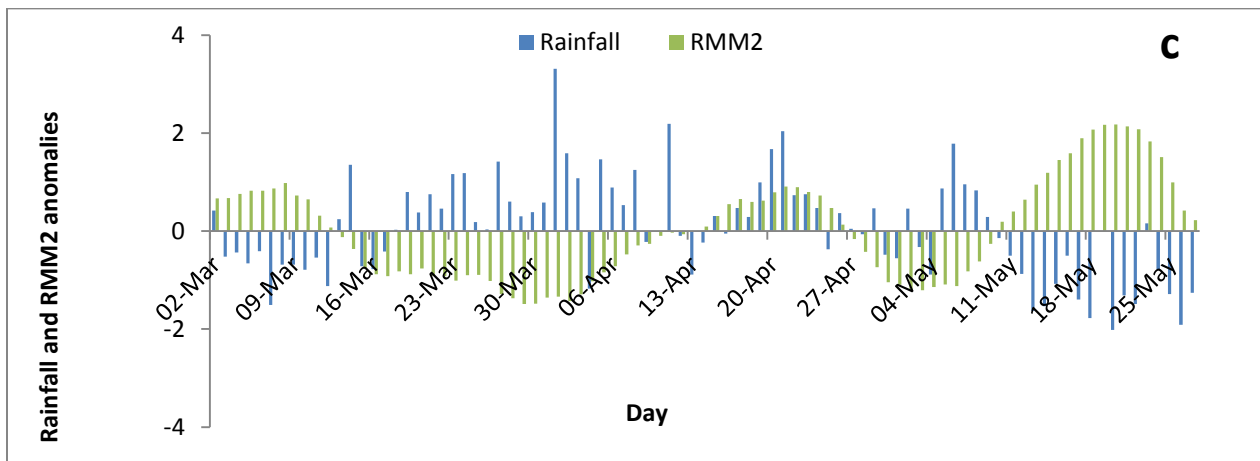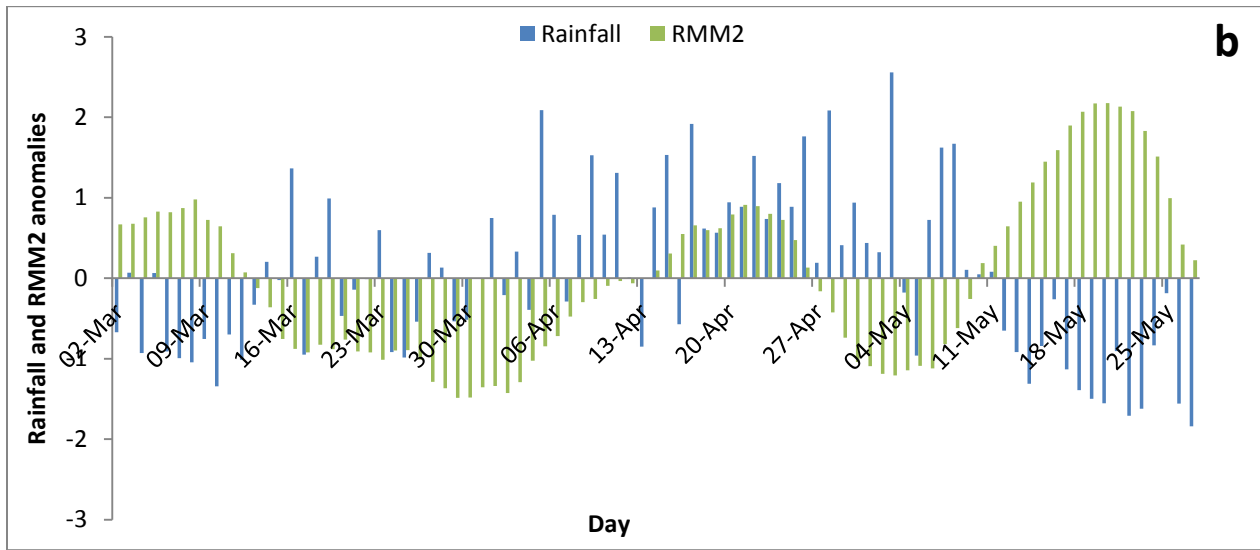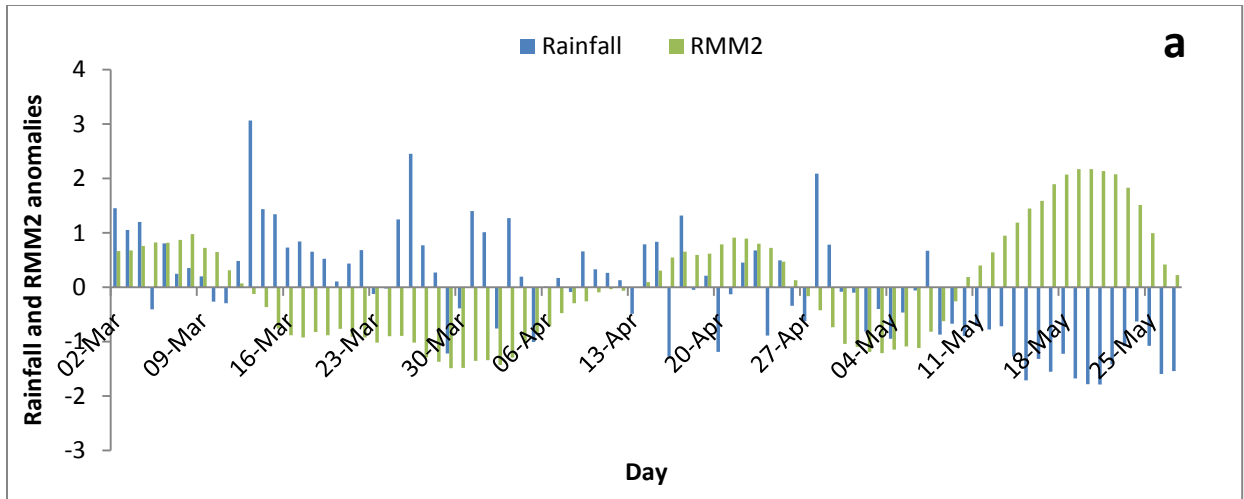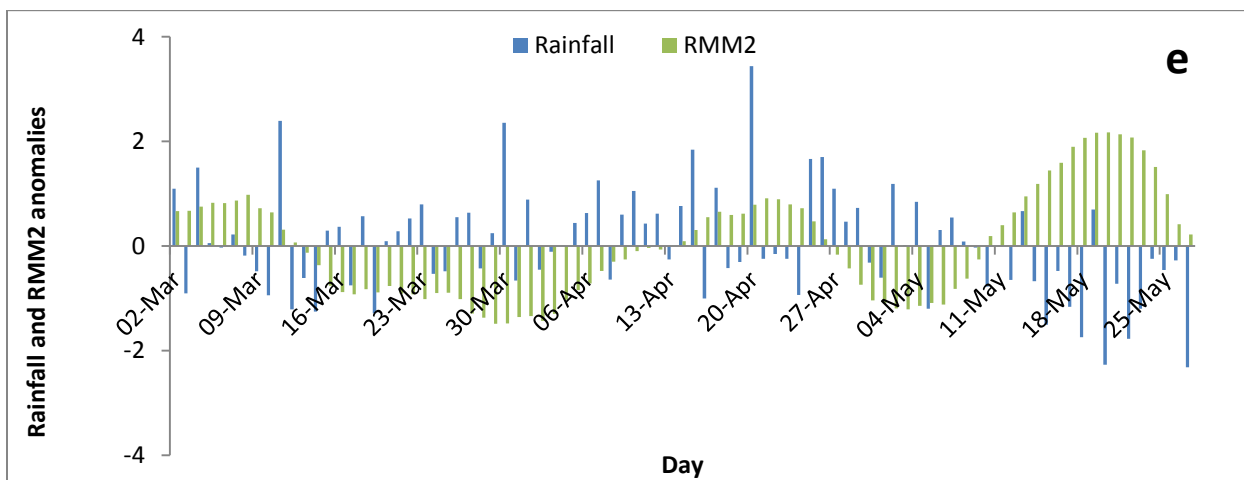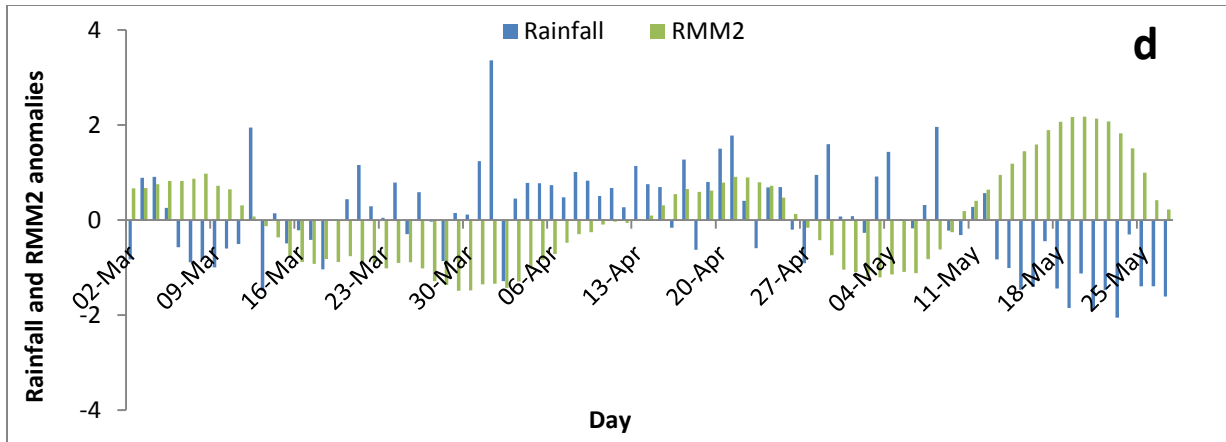
Figure 11: Daily variation of rainfall anomalies at lag five with RMM2 component at (a) Kamembe, (b) Gikongoro, (c) Kigali, (d) Byumba and (e) Kibungo stations.

Figure 12 show the daily variation of rainfall anomalies at lag five with RMM1 component over five stations.

Figure 12a shows the Daily variation of rainfall anomalies at lag zero with Wind component anomalies over Kamembe station. Figure 12a shows that enhance tendency between rainfall and wind anomalies occurs during the fourth week of March to the third week of April and from the first week to the second week of May while a depressed tendency occurs between the second to third week of March and the third to the last week of May.

Figure 12b show the Daily variation of rainfall anomalies at lag zero with Wind component anomalies over Gikongoro station. Figure 12b shows enhance tendency between rainfall and wind anomalies during the fourth week of March to the third week of April and from the first

33

week to the second week of May while a depressed tendency occurs between the first to second week of March and the second to the last week of May.

Figure 12c show the Daily variation of rainfall anomalies at lag zero with Wind component anomalies over Kigali station. Figure 11c shows enhance tendency between rainfall and wind anomalies during the fourth week of March to the third week of April and from the first week to the second week of May while a depressed tendency occurs between the first to second week of March and the third to the last week of May.

Figure 12d show the Daily variation of rainfall anomalies at lag zero with Wind component anomalies over Byumba station. Figure 11d shows enhance tendency between rainfall and wind anomalies during the fourth week of March to the third week of April and from the first week to the second week of May while a depressed tendency occurs between the second to third week of March and the third to the last week of May.

 Figure 12e shows the Daily variation of rainfall anomalies at lag zero with Wind component anomalies over Kibungo station. Figure 11e shows enhance tendency between rainfall and wind anomalies during the fourth week of March to the third week of April and from the second week to the third week of May while a depressed tendency occurs between the second to third week of March and the last two weeks of May.

34
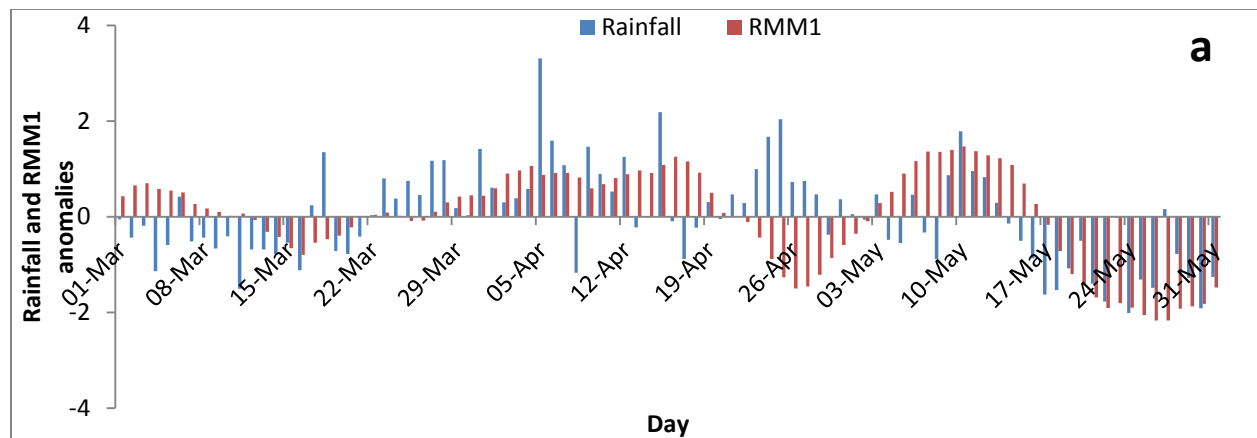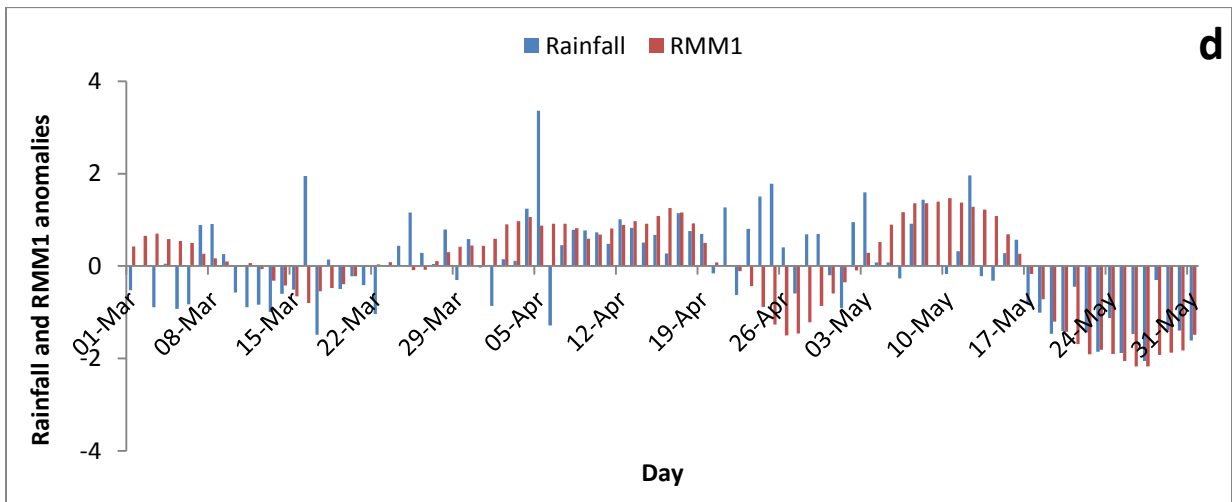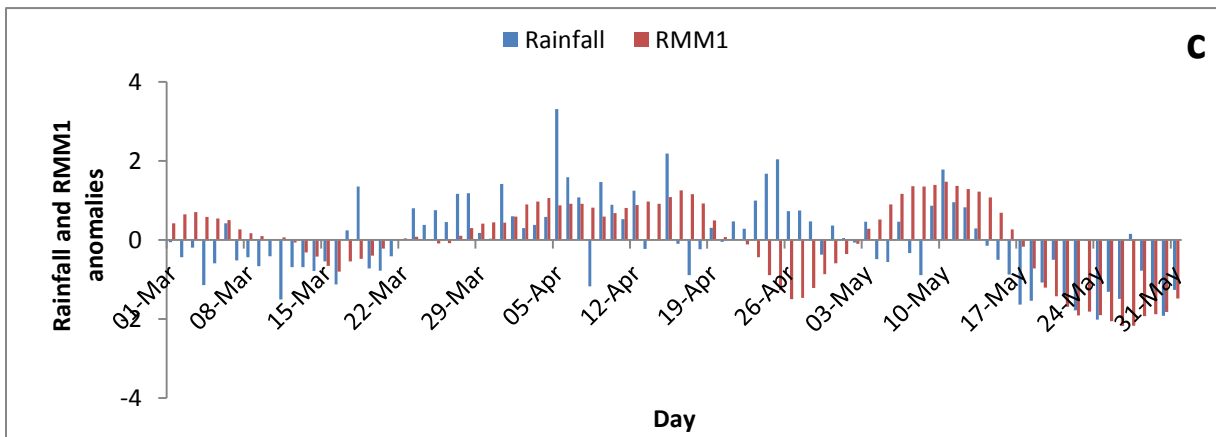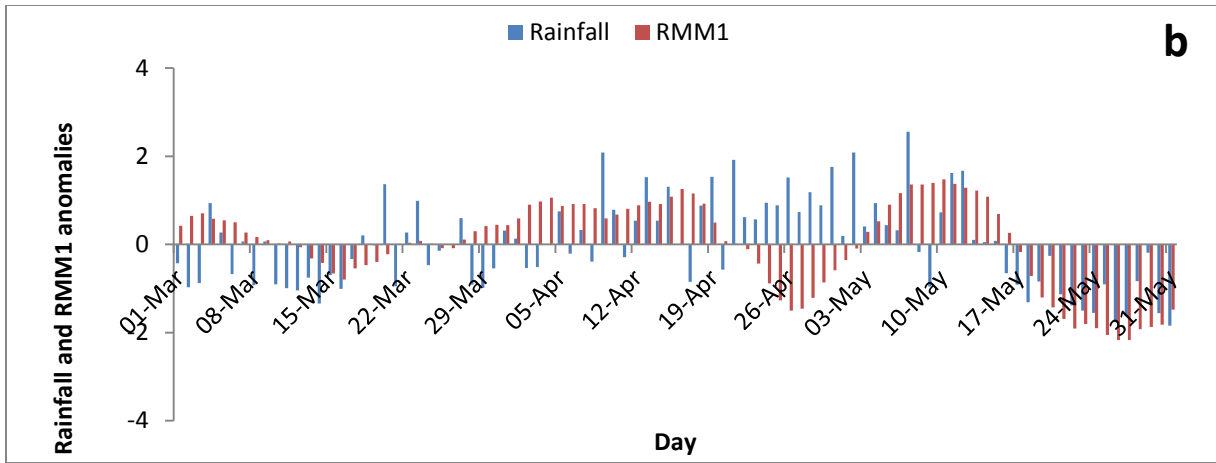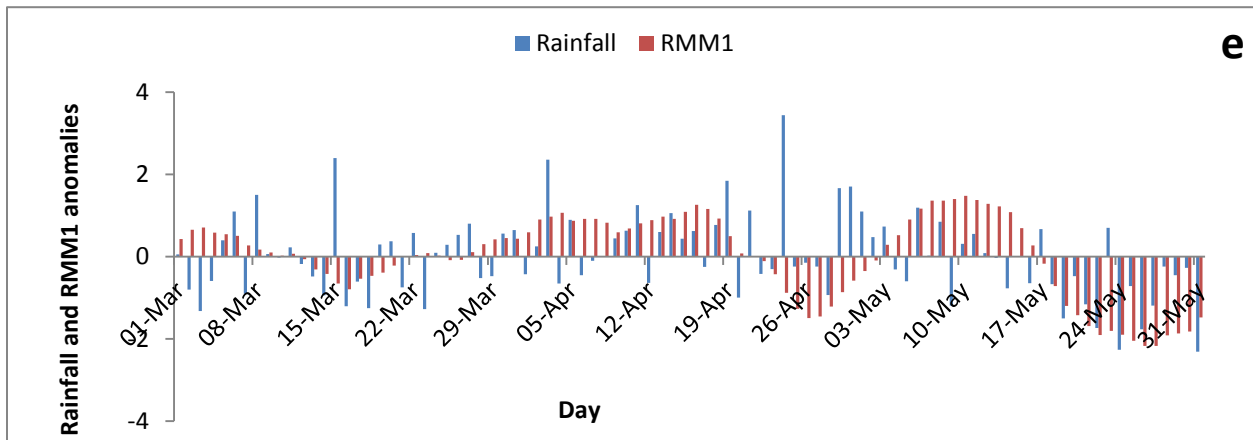
Figure 12: Daily variation of rainfall anomalies at lag zero with RMM1 component at (a), Kamembe, (b) Gikongoro, (c) Kigali, (d) Byumba and (e) Kibungo stations.

5.4 Correlation analysis

The degree of association between MJO indices with daily rainfall can be assessed using correlation. In this study simple correlation is used to determine the degree of association between Madden-Julian Oscillation (MJO) indices and daily rainfall. Lag linear correlation between daily rainfall anomalies and MJO indices was performed to establish its relationship with rainfall. Maximum positive correlation (0.50) between rainfall and RMM1 indices occurs at lag zero while a maximum negative correlation (-0.43) between rainfall and RMM2 indices occurs at lag five positive. The explained variance between rainfall and the MJO is obtained by squaring the correlation coefficient. The highest variance explained is 25% with the RMM1 indices and a variance of 18.6% with RMM2 indices.

Figure13a shows the correlation between rainfall and RMM1 indices at lag zero. The figure shows that rainfall and wind indices have a significant positive correlation at lag zero.

Figure13b shows the correlation between rainfall with RMM2 indices at different lag time. The figure shows that rainfall and OLR indices have a significant negative correlation at lag five
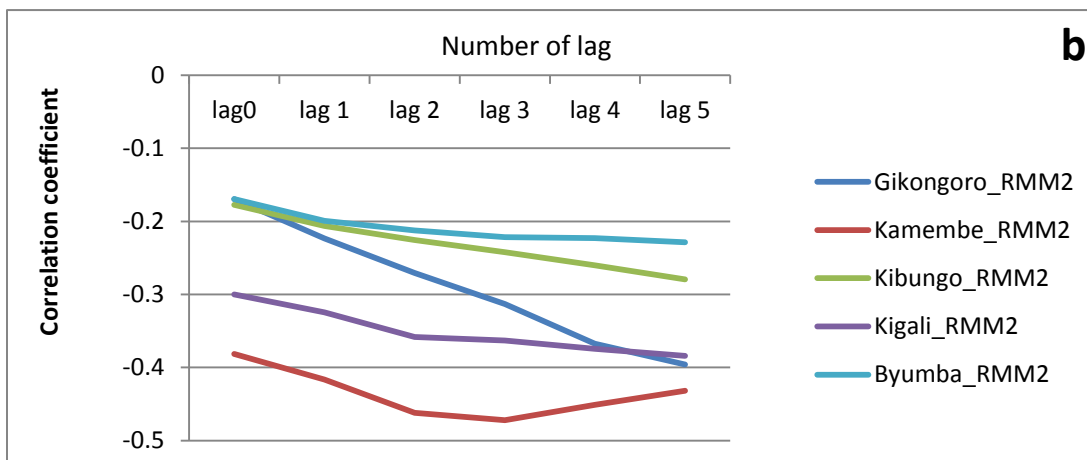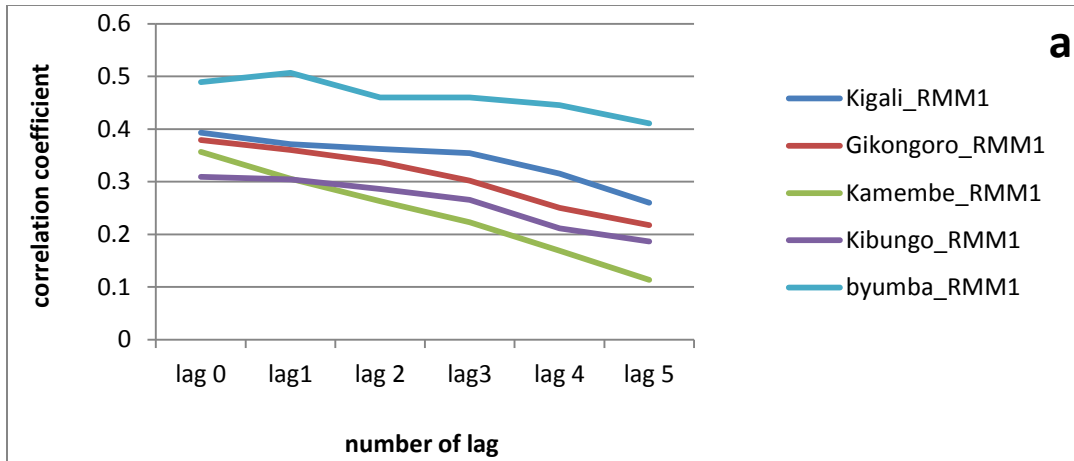
Figure13: Correlation of rainfall at different lag time during MAM season with (a) RMM1 indices and (b) RMM2 indices.

5.5 Conclusion and Recommendations

5.5.1 Conclusion

The temporal and spatial analysis indicated that the rainfall peaks during the first two weeks of March starting from the western and southern part moving to northern and central and then to eastern part with high rainfall over the southern and western part of the country. The high frequency of rain days is located from the third week of March to the second week of May.

The considerable number of wet spells during MAM season are located between the third week of March to the second week of May and the days of the season with high number of wet spells while dry spells are located within the last two weeks of May. Composite of rainfall anomalies

with OLR anomalies indicate a well-established opposite pattern between the rainfall anomalies and the OLR component anomalies at lag five while a positive pattern between rainfall anomalies and wind component anomalies is established at lag zero

The degree of association between MJO indices with daily rainfall can be assessed using correlation. The correlations are performed for all stations used in this study. Maximum negative correlation(-0.43) between rainfall and OLR component occurs at lag five while a maximum positive correlation(0.50) between rainfall and wind component occurs at lag zero. The explained variance between rainfall and the MJO is obtained by squaring the correlation coefficient. The highest variance explained is 18.6% with OLR component and a variance of 25% with the wind component. The same correlations are observed using the anomalies.

Therefore, the study reveals an association between Madden-Julian Oscillation and Wet and Dry spells over Rwanda. The prediction of rainfall on intra-seasonal timescales can be improved by using the MJO patterns over Rwanda.

5.5.2 Recommendation

The study used mainly the composite and correlation method between rainfall and MJO indices for the long rain season (MAM). It is recommended that further study can be done for the short rain season.

The study focused on the association between the rainfall and MJO indices. It is recommended that other meteorological parameters such as wind at various levers and mean sea level pressure be investigated. The study reveals that only 25% of variance is explained by using the MJO as predictor of rainfall at intra-seasonal rainfall time scale. It is recommended that the association between intra-seasonal rainfall and other mode of variability such as Sea Surface Temperature (SST) and the Indian Ocean Dipole (IOD) be investigated.

Table 1: Summary of Daily Mean Rainfall and MJO.

	Stations names					**MJO indices**	
Days							
	Kigali	Kibungo	Kamembe	Byumba	Gikongoro	RMM1	RMM2
01-Mar	4.028571	4.36	5.72	3.32	4.28142857	0.062806	0.202862
02-Mar	3.34	2.798571	7.24	4.185714	2.92357143	0.116172	0.204651
03-Mar	3.782857	1.855457	4	2.731429	3.15145143	0.128457	0.226257
04-Mar	2.085714	3.183171	4.788571	4.248571	7.66457143	0.100165	0.244581
05-Mar	3.068571	4.981429	7.336	2.671429	6.01451429	0.091389	0.243275
06-Mar	4.877143	6.253371	7.634857	2.825714	3.67131429	0.081602	0.25649
07-Mar	3.197143	2.618429	6.865714	5.6	5.50937143	0.02632	0.284772
08-Mar	3.345714	6.985714	7.144286	5.634286	3.03234286	0.003706	0.217679
09-Mar	2.942857	4.361429	4.048571	4.585714	5.49662857	-0.01365	0.196668
10-Mar	3.388571	4.212857	6.382857	3.242857	3.08148571	-0.03168	0.108516
11-Mar	1.431429	4.667143	5.305714	2.725714	2.86765714	-0.02109	0.044887
12-Mar	2.897143	3.925714	5.511143	2.82	2.74154286	-0.05195	-0.00703
13-Mar	2.899429	3.385571	5.220412	2.56	3.46228571	-0.11032	-0.07027
14-Mar	2.717143	2.548571	4.325714	3.197143	2.00365714	-0.13541	-0.17421
15-Mar	3.156571	8.603714	4.270286	3.345714	3.60662857	-0.1902	-0.20707
16-Mar	2.12	2.0648	5.768286	7.311429	2.82705882	-0.22335	-0.21837
17-Mar	4.56	3.15	10.74343	1.76	4.51888235	-0.16311	-0.19256
18-Mar	6.548571	1.985143	7.6	4.391429	5.84468571	-0.14718	-0.20805
19-Mar	2.84	4.794686	7.414286	3.368571	5.28434286	-0.12881	-0.17599
20-Mar	2.734286	4.928571	6.244571	3.814286	8.72594286	-0.08803	-0.21524
21-Mar	3.382857	2.8976	6.46	3.494286	2.97977143	-0.03898	-0.21801
22-Mar	4.18	5.298686	6.097143	2.485714	6.00114286	-0.02704	-0.2428
23-Mar	5.56	1.933771	5.837143	4.171429	7.80011429	-0.01667	-0.21239
24-Mar	4.808571	4.430714	5.037143	4.871429	4.17577143	-0.0324	-0.21036
25-Mar	5.471429	4.772457	5.671429	6.037143	4.98211429	-0.05667	-0.2429
26-Mar	4.942857	5.212686	6.149714	4.631429	5.30914286	-0.0557	-0.31529
27-Mar	6.217143	5.706923	4.597143	4.24	6.81645714	-0.01105	-0.33651
28-Mar	6.242857	3.301714	4.782857	5.442857	3.06291429	0.034242	-0.36773
29-Mar	4.451429	3.387714	7.235429	3.682857	2.89097143	0.061635	-0.36658
30-Mar	4.188571	5.267657	9.557143	5.114286	3.99222857	0.067971	-0.33299
31-Mar	6.665714	5.421429	6.317143	4.108571	6.12125714	0.06593	-0.32855
01-Apr	5.208571	3.481143	5.349714	2.767647	5.66034286	0.102149	-0.3521
02-Apr	4.662857	4.712314	2.488571	4.405882	4.00571429	0.174654	-0.31644
03-Apr	4.817143	8.534429	4.085143	4.35	4.05828235	0.191125	-0.24524
04-Apr	5.168571	3.068029	7.528571	6.170588	5.32857143	0.212875	-0.1977

Days	Stations names					MJO indices	
	Kigali	Kibungo	Kamembe	Byumba	Gikongoro	RMM1	RMM2
05-Apr	10.06	5.873029	6.78	9.6	7.19182857	0.16807	-0.16403
06-Apr	6.974286	3.438743	3.371429	2.088235	4.81142857	0.178579	-0.10017
07-Apr	6.057143	4.064366	7.284	4.897059	6.15434286	0.177912	-0.05244
08-Apr	2.022857	4.263074	5.213143	5.435294	4.36085714	0.155801	-0.04228
09-Apr	6.754286	5.062	2.897143	5.414706	10.52	0.102163	0.000709
10-Apr	5.725714	5.405317	4.854286	5.35	7.29571429	0.122676	0.017009
11-Apr	5.071429	6.535971	5.165143	4.938235	4.62171429	0.153253	0.009061
12-Apr	6.368571	3.097051	4.66	5.802941	6.66742857	0.171237	0.023861
13-Apr	3.727143	5.349457	6.101143	5.505882	9.12571429	0.190824	0.051039
14-Apr	4.105714	6.174029	5.471429	4.982353	6.68088	0.177567	0.107621
15-Apr	8.048571	5.044143	5.340571	5.258824	8.58357143	0.217438	0.171352
16-Apr	3.954286	5.383029	5.088286	4.602941	5.35428571	0.25792	0.19955
17-Apr	2.54	3.799457	3.888286	6.011765	3.22489143	0.234936	0.183543
18-Apr	3.711429	5.654686	6.348571	5.385294	7.51737143	0.180101	0.190359
19-Apr	4.674286	7.602574	6.442857	5.294118	9.14251429	0.080361	0.235333
20-Apr	4.04	2.4426	2.373429	3.908824	3.91505714	-0.01839	0.267274
21-Apr	4.965714	6.2826	7.371429	6.223529	10.0984343	-0.03301	0.262469
22-Apr	4.642857	3.499	4.746286	3.152941	6.86605714	-0.06159	0.237269
23-Apr	5.911429	3.705971	5.244571	5.467647	6.73714286	-0.1381	0.217628
24-Apr	7.125714	10.50571	2.542857	6.597059	7.68285714	-0.24365	0.150882
25-Apr	7.782857	3.823857	4.582857	7.041176	7.54371429	-0.33319	0.060801
26-Apr	5.434286	3.980886	5.705143	4.823529	9.11211429	-0.38758	-0.01679
27-Apr	5.468571	3.820886	6.132286	3.208824	7.16828571	-0.37868	-0.08634
28-Apr	4.968571	2.563143	3.117143	5.279412	8.27514286	-0.32084	-0.16941
29-Apr	3.457143	7.284286	5.791429	5.291176	7.53782857	-0.23903	-0.24995
30-Apr	4.78	7.346466	4.18	3.844118	9.70914286	-0.17456	-0.26401
01-May	4.216286	6.251286	3.631429	2.7	5.81371429	-0.11912	-0.28921
02-May	4.011429	5.110286	8.854286	5.7	10.5072771	-0.05851	-0.29413
03-May	4.960857	5.582314	6.338286	6.744118	6.35804571	0.031056	-0.27709
04-May	3.259429	3.690641	4.674571	4.291176	7.66857143	0.085705	-0.26262
05-May	3.136286	3.163143	4.641143	4.297059	6.42949714	0.174066	-0.27068
06-May	4.952286	6.412343	3.266	3.735294	6.1384	0.236274	-0.19112
07-May	3.538571	4.301314	4.060571	5.647059	11.6851714	0.282469	-0.1383
08-May	2.540171	5.794114	3.008571	6.488235	4.8988	0.281399	-0.04257
09-May	5.686571	2.088857	3.938857	4.2	2.95282857	0.290885	0.076014
10-May	7.324571	4.814657	4.725714	3.888235	7.13774286	0.308622	0.132216
11-May	5.840286	5.254	6.129143	4.679412	9.36648571	0.284996	0.196416
12-May	5.615714	4.413686	3.157714	7.335294	9.482	0.264556	0.277482
13-May	4.647714	4.202314	3.542857	3.811765	5.59714286	0.250014	0.340875

40

Days	Stations names					MJO indices	
	Kigali	Kibungo	Kamembe	Byumba	Gikongoro	RMM1	RMM2
14-May	3.868571	2.849714	3.108	3.652941	5.45714286	0.217097	0.409423
15-May	3.226571	4.2656	3.456571	4.617647	5.536	0.125495	0.447259
16-May	2.564857	3.083743	3.34	5.085294	3.72	0.025996	0.528259
17-May	1.207429	5.473583	3.449714	2.826471	3.06028571	-0.07644	0.574126
18-May	1.373714	3.037686	2.369143	2.535294	2.08305714	-0.20491	0.600567
19-May	2.197143	1.531414	1.535429	1.794118	3.24571429	-0.31796	0.601563
20-May	3.225714	3.398171	2.294286	1.894118	4.68857143	-0.37049	0.590935
21-May	1.622857	2.155171	1.841429	3.447059	2.52285714	-0.43221	0.57593
22-May	0.943143	1.102257	2.470286	1.838235	1.88857143	-0.48313	0.509969
23-May	4.088571	5.527229	1.605143	1.173529	1.61582857	-0.46021	0.426183
24-May	0.518	0.137143	1.394118	2.347059	1.48	-0.48205	0.289493
25-May	1.776286	2.957143	1.382286	1.123529	3.08908571	-0.51712	0.136297
26-May	1.458857	1.0476	2.106857	1.785294	1.09062857	-0.54498	0.085247
27-May	4.407714	2.091563	2.745143	0.841176	1.30777143	-0.54492	0.036316
28-May	2.739143	3.819029	3.625714	3.673529	3.26874286	-0.48622	-0.01921
29-May	1.828571	3.431057	2.756857	1.911765	4.87168571	-0.47498	-0.07381
30-May	0.697429	3.759714	1.766286	1.911765	1.46571429	-0.46342	-0.14596
31-May	1.874286	0.057143	1.868571	1.561765	0.76857143	-0.38362	-0.17147

Table 2: Summary of Daily Rainfall Anomalies and MJO indices at Lag Zero

			Station name			MJO indices	
Days	Kigali	Kibungo	Kamembe	Byumba	Gikongoro	RMM1	RMM2
01-Mar	-0.05474	0.055218	0.460792	-0.52333	-0.42518	0.423344	0.668531
02-Mar	-0.43906	-0.8049	1.249474	0.01229	-0.97221	0.651204	0.675284
03-Mar	-0.19189	-1.32441	-0.43166	-0.88748	-0.8804	0.70366	0.756867
04-Mar	-1.13912	-0.59304	-0.0225	0.05118	0.937754	0.582858	0.82606
05-Mar	-0.59055	0.397532	1.299286	-0.9246	0.273012	0.545386	0.821128
06-Mar	0.418875	1.098183	1.454354	-0.82914	-0.67097	0.5036	0.871029
07-Mar	-0.51879	-0.90413	1.055269	0.887309	0.06951	0.267557	0.977822
08-Mar	-0.43587	1.501595	1.199811	0.908521	-0.92839	0.171	0.724477
09-Mar	-0.66072	0.056005	-0.40646	0.25977	0.064376	0.096911	0.645139
10-Mar	-0.41195	-0.02584	0.804729	-0.57106	-0.90859	0.01993	0.312281
11-Mar	-1.5043	0.224408	0.245832	-0.89101	-0.99473	0.065128	0.072017
12-Mar	-0.68623	-0.18401	0.352422	-0.83268	-1.04554	-0.06663	-0.12404
13-Mar	-0.68496	-0.48155	0.201571	-0.99354	-0.75518	-0.31587	-0.36282
14-Mar	-0.7867	-0.94261	-0.26266	-0.59934	-1.3428	-0.42301	-0.75528
15-Mar	-0.54144	2.392872	-0.29142	-0.50742	-0.69703	-0.65695	-0.87938

16-Mar	-1.11999	-1.2091	0.485846	1.94617	-1.01109	-0.79846	-0.92203
17-Mar	0.241866	-0.61131	3.067298	-1.4885	-0.32952	-0.54127	-0.82459
18-Mar	1.351759	-1.25297	1.436268	0.139565	0.204595	-0.47326	-0.88309
19-Mar	-0.71813	0.294665	1.339906	-0.49328	-0.02115	-0.39482	-0.76201
20-Mar	-0.77713	0.368416	0.732976	-0.21751	1.365338	-0.2207	-0.91023
21-Mar	-0.41514	-0.75035	0.844756	-0.4155	-0.94956	-0.01125	-0.92069
22-Mar	0.029774	0.572294	0.65648	-1.0395	0.267625	0.039702	-1.01428
23-Mar	0.800002	-1.28127	0.521574	0.003451	0.992359	0.084006	-0.89945
24-Mar	0.380603	0.094171	0.106478	0.436541	-0.46774	0.016853	-0.89178
25-Mar	0.750567	0.28242	0.43559	1.157769	-0.1429	-0.08679	-1.01465
26-Mar	0.455552	0.524921	0.683758	0.288053	-0.01115	-0.08267	-1.288
27-Mar	1.166777	0.797172	-0.12182	0.045876	0.596082	0.10798	-1.36815
28-Mar	1.181129	-0.52774	-0.02546	0.790084	-0.91607	0.301381	-1.48604
29-Mar	0.181268	-0.48037	1.247102	-0.29883	-0.98534	0.418343	-1.4817
30-Mar	0.034558	0.555202	2.45177	0.586797	-0.54169	0.445397	-1.35486
31-Mar	1.417141	0.639907	0.770632	-0.03544	0.316014	0.436682	-1.33807
01-Apr	0.603857	-0.4289	0.268662	-0.86507	0.13033	0.591328	-1.42703
02-Apr	0.299274	0.24929	-1.2159	0.148508	-0.53625	0.900909	-1.29234
03-Apr	0.385387	2.354706	-0.38749	0.113933	-0.51508	0.97124	-1.02351
04-Apr	0.581532	-0.65647	1.399205	1.240332	-0.00333	1.064106	-0.844
05-Apr	3.311614	0.888671	1.010794	3.36211	0.747305	0.872798	-0.71684
06-Apr	1.589366	-0.45226	-0.75781	-1.28542	-0.21166	0.917668	-0.47573
07-Apr	1.077475	-0.10763	1.272305	0.452399	0.329343	0.914821	-0.29548
08-Apr	-1.1742	0.001826	0.197799	0.785405	-0.39318	0.82041	-0.25711
09-Apr	1.466576	0.441915	-1.0039	0.772667	2.088092	0.59139	-0.0948
10-Apr	0.892493	0.631032	0.011599	0.732634	0.789156	0.678975	-0.03325
11-Apr	0.527313	1.253854	0.172893	0.477875	-0.28809	0.809531	-0.06326
12-Apr	1.251295	-0.64048	-0.08921	1.012868	0.536045	0.886322	-0.00738
13-Apr	-0.22298	0.600261	0.658556	0.829078	1.52639	0.969953	0.095244
14-Apr	-0.01169	1.054477	0.331816	0.50517	0.541464	0.913349	0.308899
15-Apr	2.188963	0.432079	0.263918	0.676223	1.307982	1.08359	0.549548
16-Apr	-0.0962	0.618754	0.133015	0.270428	0.007032	1.256437	0.656025
17-Apr	-0.88557	-0.25356	-0.48963	1.142068	-0.85082	1.158301	0.595581
18-Apr	-0.23175	0.768397	0.786939	0.75447	0.878453	0.924167	0.621317
19-Apr	0.305653	1.841393	0.835861	0.698059	1.533158	0.498298	0.791141
20-Apr	-0.04836	-1.00098	-1.27564	-0.15902	-0.57278	0.07664	0.911749
21-Apr	0.46831	1.114284	1.317669	1.273087	1.91826	0.014238	0.893604
22-Apr	0.288112	-0.41907	-0.04444	-0.62669	0.616064	-0.10779	0.798452
23-Apr	0.996147	-0.30505	0.214107	0.805422	0.56413	-0.43448	0.724287
24-Apr	1.673883	3.440591	-1.18773	1.504189	0.94512	-0.88516	0.472253
25-Apr	2.040658	-0.24012	-0.12924	1.778965	0.889065	-1.26747	0.132108

26-Apr	0.729836	-0.15362	0.453083	0.406906	1.520911	-1.49969	-0.16088
27-Apr	0.748972	-0.24175	0.674715	-0.59211	0.73782	-1.4617	-0.42351
28-Apr	0.469904	-0.93458	-0.88975	0.688961	1.183729	-1.21475	-0.73718
29-Apr	-0.37368	1.666064	0.497854	0.69624	0.886694	-0.86544	-1.0413
30-Apr	0.364656	1.700316	-0.33827	-0.19906	1.76143	-0.59016	-1.09439
01-May	0.050027	1.097034	-0.6229	-0.90692	0.192117	-0.35342	-1.18953
02-May	-0.06431	0.468513	2.087079	0.949179	2.082966	-0.09467	-1.20811
03-May	0.465599	0.728531	0.781602	1.595175	0.411407	0.28778	-1.14377
04-May	-0.48403	-0.3135	-0.08165	0.077539	0.939365	0.521119	-1.08913
05-May	-0.55276	-0.60407	-0.09899	0.081179	0.440192	0.898398	-1.11955
06-May	0.460815	1.185753	-0.81251	-0.26639	0.32292	1.164012	-0.81916
07-May	-0.32823	0.022891	-0.40024	0.916424	2.557493	1.361258	-0.61972
08-May	-0.88547	0.845201	-0.94609	1.43686	-0.17646	1.356689	-0.25823
09-May	0.870646	-1.19584	-0.46339	0.021128	-0.96042	1.397191	0.18955
10-May	1.784873	0.305666	-0.05511	-0.17176	0.725516	1.472925	0.401769
11-May	0.956439	0.547679	0.673084	0.317741	1.623387	1.372048	0.644188
12-May	0.831098	0.084791	-0.8687	1.960936	1.669923	1.284773	0.950297
13-May	0.290822	-0.03164	-0.66886	-0.21907	0.10487	1.222683	1.189668
14-May	-0.14405	-0.77672	-0.8945	-0.31734	0.048469	1.082135	1.448504
15-May	-0.50237	0.003217	-0.71363	0.279527	0.080238	0.691011	1.591374
16-May	-0.87169	-0.64781	-0.77412	0.56886	-0.65136	0.266174	1.897229
17-May	-1.62932	0.668636	-0.71719	-0.82867	-0.91713	-0.1712	2.070423
18-May	-1.53651	-0.67318	-1.27787	-1.00883	-1.31082	-0.71973	2.170264
19-May	-1.07693	-1.50291	-1.71046	-1.46739	-0.84243	-1.20245	2.174028
20-May	-0.50285	-0.47461	-1.31671	-1.40552	-0.26116	-1.42673	2.133894
21-May	-1.39746	-1.15931	-1.55168	-0.44472	-1.13364	-1.69025	2.077236
22-May	-1.77683	-1.73931	-1.22539	-1.4401	-1.38917	-1.9077	1.828165
23-May	-0.02126	0.698187	-1.67428	-1.85135	-1.49904	-1.80983	1.511789
24-May	-2.01412	-2.27095	-1.78378	-1.12529	-1.55376	-1.90305	0.99565
25-May	-1.31183	-0.71755	-1.78992	-1.88228	-0.90553	-2.05281	0.417179
26-May	-1.48899	-1.76942	-1.41396	-1.47285	-1.71062	-2.17178	0.224414
27-May	0.15687	-1.19435	-1.08277	-2.05698	-1.62315	-2.17153	0.03965
28-May	-0.77442	-0.24278	-0.62587	-0.3046	-0.83315	-1.92088	-0.17002
29-May	-1.28264	-0.45649	-1.07669	-1.3946	-0.18739	-1.8729	-0.37619
30-May	-1.91397	-0.27545	-1.59067	-1.3946	-1.55952	-1.82352	-0.64864
31-May	-1.25713	-2.31502	-1.5376	-1.61115	-1.84037	-1.4828	-0.74496

Table 3: Summary of Daily Rainfall Anomalies and MJO indices at Lag five

Days	Station name					MJO indices	
	Kigali	Kibungo	Kamembe	Byumba	Gikongoro	RMM1	RMM2
01-Mar	0.418875	1.098183	1.45435391	-0.82914	-0.670969774	0.423344	0.668531
02-Mar	-0.51879	-0.90413	1.05526883	0.887309	0.069509924	0.651204	0.675284
03-Mar	-0.43587	1.501595	1.19981116	0.908521	-0.928385803	0.70366	0.756867
04-Mar	-0.66072	0.056005	-0.40646182	0.25977	0.064376337	0.582858	0.82606
05-Mar	-0.41195	-0.02584	0.80472879	-0.57106	-0.908588112	0.545386	0.821128
06-Mar	-1.5043	0.224408	0.24583177	-0.89101	-0.99473109	0.5036	0.871029
07-Mar	-0.68623	-0.18401	0.35242248	-0.83268	-1.045537491	0.267557	0.977822
08-Mar	-0.68496	-0.48155	0.20157086	-0.99354	0.755179024	0.171	0.724477
09-Mar	-0.7867	-0.94261	-0.26266073	-0.59934	-1.342802129	0.096911	0.645139
10-Mar	-0.54144	2.392872	-0.29142095	-0.50742	-0.697029061	0.01993	0.312281
11-Mar	-1.11999	-1.2091	0.48584617	1.94617	-1.011086529	0.065128	0.072017
12-Mar	0.241866	-0.61131	3.06729807	-1.4885	-0.329518504	-0.06663	-0.12404
13-Mar	1.351759	-1.25297	1.43626758	0.139565	0.204594637	-0.31587	-0.36282
14-Mar	-0.71813	0.294665	1.33990603	-0.49328	-0.021145086	-0.42301	-0.75528
15-Mar	-0.77713	0.368416	0.73297649	-0.21751	1.365337886	-0.65695	-0.87938
16-Mar	-0.41514	-0.75035	0.84475589	-0.4155	-0.949564729	-0.79846	-0.92203
17-Mar	0.029774	0.572294	0.65648024	-1.0395	0.267624961	-0.54127	-0.82459
18-Mar	0.800002	-1.28127	0.52157407	0.003451	0.992358589	-0.47326	-0.88309
19-Mar	0.380603	0.094171	0.10647814	0.436541	-0.46774417	-0.39482	-0.76201
20-Mar	0.750567	0.28242	0.43558991	1.157769	-0.142900888	-0.2207	-0.91023
21-Mar	0.455552	0.524921	0.68375797	0.288053	-0.011154158	-0.01125	-0.92069
22-Mar	1.166777	0.797172	-0.12182462	0.045876	0.596082473	0.039702	-1.01428
23-Mar	1.181129	-0.52774	-0.02546306	0.790084	-0.916069798	0.084006	-0.89945
24-Mar	0.181268	-0.48037	1.24710244	-0.29883	-0.985338697	0.016853	-0.89178
25-Mar	0.034558	0.555202	2.45177011	0.586797	-	-0.08679	-1.01465

44

					0.541686245		
26-Mar	1.417141	0.639907	0.77063162	-0.03544	0.316014202	-0.08267	-1.288
27-Mar	0.603857	-0.4289	0.26866205	-0.86507	0.130330274	0.10798	-1.36815
28-Mar	0.299274	0.24929	-1.21589887	0.148508	-0.536253391	0.301381	-1.48604
29-Mar	0.385387	2.354706	0.38748601	0.113933	-0.515075819	0.418343	-1.4817
30-Mar	0.581532	-0.65647	1.39920545	1.240332	-0.003327164	0.445397	-1.35486
31-Mar	3.311614	0.888671	1.01079426	3.36211	0.747304607	0.436682	-1.33807
01-Apr	1.589366	-0.45226	0.75781087	-1.28542	-0.211663334	0.591328	-1.42703
02-Apr	1.077475	-0.10763	1.27230469	0.452399	0.329343113	0.900909	-1.29234
03-Apr	-1.1742	0.001826	0.19779925	0.785405	-0.39318054	0.97124	-1.02351
04-Apr	1.466576	0.441915	-1.00390345	0.772667	2.088091745	1.064106	-0.844
05-Apr	0.892493	0.631032	0.01159907	0.732634	0.789156006	0.872798	-0.71684
06-Apr	0.527313	1.253854	0.17289349	0.477875	-0.288091631	0.917668	-0.47573
07-Apr	1.251295	-0.64048	-0.08920994	1.012868	0.536044823	0.914821	-0.29548
08-Apr	-0.22298	0.600261	0.65855572	0.829078	1.526389803	0.82041	-0.25711
09-Apr	-0.01169	1.054477	0.33181593	0.50517	0.541463866	0.59139	-0.0948
10-Apr	2.188963	0.432079	0.2639181	0.676223	1.307982133	0.678975	-0.03325
11-Apr	-0.0962	0.618754	0.13301463	0.270428	0.007032093	0.809531	-0.06326
12-Apr	-0.88557	-0.25356	-0.48962925	1.142068	-0.850815686	0.886322	-0.00738
13-Apr	-0.23175	0.768397	0.78693896	0.75447	0.878452802	0.969953	0.095244
14-Apr	0.305653	1.841393	0.83586098	0.698059	1.533157851	0.913349	0.308899
15-Apr	-0.04836	-1.00098	-1.27564304	-0.15902	-0.572775527	1.08359	0.549548
16-Apr	0.46831	1.114284	1.31766875	1.273087	1.918259781	1.256437	0.656025
17-Apr	0.288112	-0.41907	-0.04443888	-0.62669	0.616064329	1.158301	0.595581
18-Apr	0.996147	-0.30505	0.21410659	0.805422	0.56412992	0.924167	0.621317
19-Apr	1.673883	3.440591	1.18773165	1.504189	0.945120376	0.498298	0.791141
20-Apr	2.040658	-0.24012	-0.12923704	1.778965	0.889065285	0.07664	0.911749
21-Apr	0.729836	-0.15362	0.45308324	0.406906	1.520910907	0.014238	0.893604
22-Apr	0.748972	-0.24175	0.67471481	-0.59211	0.737820131	-0.10779	0.798452
23-Apr	0.469904	-0.93458	-0.88975207	0.688961	1.183728599	-0.43448	0.724287
24-Apr	-0.37368	1.666064	0.4978543	0.69624	0.886694166	-0.88516	0.472253

Date							
25-Apr	0.364656	1.700316	-0.33826749	-0.19906	1.761429837	-1.26747	0.132108
26-Apr	0.050027	1.097034	-0.6229047	-0.90692	0.192117487	-1.49969	-0.16088
27-Apr	-0.06431	0.468513	2.08707869	0.949179	2.082966214	-1.4617	-0.42351
28-Apr	0.465599	0.728531	0.78160201	1.595175	0.411406846	-1.21475	-0.73718
29-Apr	-0.48403	-0.3135	-0.08164926	0.077539	0.939365234	-0.86544	-1.0413
30-Apr	-0.55276	-0.60407	-0.09899434	0.081179	0.440191768	-0.59016	-1.09439
01-May	0.460815	1.185753	-0.81251458	-0.26639	0.322920374	-0.35342	-1.18953
02-May	-0.32823	0.022891	-0.40023538	0.916424	2.557492705	-0.09467	-1.20811
03-May	-0.88547	0.845201	-0.94608652	1.43686	-0.176464881	0.28778	-1.14377
04-May	0.870646	-1.19584	-0.46338926	0.021128	-0.960418928	0.521119	-1.08913
05-May	1.784873	0.305666	-0.05511277	-0.17176	0.725515636	0.898398	-1.11955
06-May	0.956439	0.547679	0.67308408	0.317741	1.623386981	1.164012	-0.81916
07-May	0.831098	0.084791	-0.86870078	1.960936	1.669923066	1.361258	-0.61972
08-May	0.290822	-0.03164	-0.66886174	-0.21907	0.104869522	1.356689	-0.25823
09-May	-0.14405	-0.77672	-0.89449603	-0.31734	0.048469122	1.397191	0.18955
10-May	-0.50237	0.003217	-0.7136328	0.279527	0.08023751	1.472925	0.401769
11-May	-0.87169	-0.64781	-0.77411821	0.56886	-0.651356247	1.372048	0.644188
12-May	-1.62932	0.668636	-0.71719077	-0.82867	-0.917128744	1.284773	0.950297
13-May	-1.53651	-0.67318	-1.27786676	-1.00883	-1.310815045	1.222683	1.189668
14-May	-1.07693	-1.50291	-1.71045602	-1.46739	-0.84242699	1.082135	1.448504
15-May	-0.50285	-0.47461	-1.31670788	-1.40552	0.261157563	0.691011	1.591374
16-May	-1.39746	-1.15931	-1.55168182	-0.44472	-1.133637217	0.266174	1.897229
17-May	-1.77683	-1.73931	-1.22538678	-1.4401	-1.38916556	-0.1712	2.070423
18-May	-0.02126	0.698187	-1.67428337	-1.85135	-1.499042747	-0.71973	2.170264
19-May	-2.01412	-2.27095	-1.783778	-1.12529	-1.553762645	-1.20245	2.174028
20-May	-1.31183	-0.71755	-	-1.88228	-	-1.42673	2.133894

			1.78991723		0.905526376		
21-May	-1.48899	-1.76942	-1.41395893	-1.47285	-1.710624818	-1.69025	2.077236
22-May	0.15687	-1.19435	-1.08277168	-2.05698	-1.623146647	-1.9077	1.828165
23-May	-0.77442	-0.24278	-0.62586967	-0.3046	0.833149699	-1.80983	1.511789
24-May	-1.28264	-0.45649	-1.07669349	-1.3946	0.187388142	-1.90305	0.99565
25-May	-1.91397	-0.27545	-1.59067119	-1.3946	1.559517788	-2.05281	0.417179
26-May	-1.25713	-2.31502	-1.53759821	-1.61115	-1.840368758	-2.17178	0.224414

Table 4: Correlation coefficients between Rainfall and RMM1

Station Name	Number of lag					
	lag 0	lag1	lag 2	lag3	lag 4	lag 5
Kigali_RMM1	0.393509	0.371636	0.362549	0.354108	0.315444	0.260372
Gikongoro_RMM1	0.379337	0.360334	0.337461	0.302024	0.250502	0.217723
Kamembe_RMM1	0.356802	0.305459	0.262941	0.22283	0.168759	0.113747
Kibungo_RMM1	0.309109	0.304777	0.286407	0.265775	0.211753	0.186625
byumba_RMM1	0.489425	0.507135	0.46002	0.46002	0.445498	0.410602

Table 5: Correlation coefficients between Rainfall and RMM2

Station Name	Number of lag					
	lag0	lag 1	lag 2	lag 3	lag 4	lag 5
Gikongoro_RMM2	-0.16921	-0.22341	-0.27079	-0.31321	-0.36722	-0.39587
Kamembe_RMM2	-0.38138	-0.41631	-0.46197	-0.47202	-0.4512	-0.43179
Kibungo_RMM2	-0.17751	-0.20622	-0.22531	-0.2422	-0.25988	-0.27942
Kigali_RMM2	-0.29992	-0.32452	-0.35829	-0.36312	-0.37436	-0.38412
Byumba_RMM2	-0.16921	-0.19903	-0.21247	-0.22173	-0.22273	-0.22849

References

Anyamba E.,1990: A diagnostic study of Low Frequency in Tropical Outgoing Long Wave radiation. Ph.D Thesis. University of California, Davis, pp.113.

Carvalho, L, C. Jones, B. Liebmann, 2004: The South Atlantic convergence zone: Intensity, Form, Persistence, and relationships with intraseasonal to interannual activity and extreme rainfall. *J. Climate*, **17,**88-108.

Hendon, H., C. Zhang, and J. Glick, 1999: Interannual variation of the Madden-Julian Oscillation during Austral summer. *J. Climate*, **12,** 2538-2550.

Higgins, W., J. Schemm, W. Shi, and A. Leetmaa, 2000: Extreme precipitation events in the western United States related to tropical forcing. *J. Climate*, **13**, 793-820.

Higgins, W and W. Shi, 2001: Intercomparison of the principal modes of interannual and intraseasonal variability of the North American monsoon system. *J. Climate*, **14**, 403-417.

Kayano, M. and V. Kousky, 1999: Intraseasonal (30-60 day) variability in the global tropics: principal modes and their evolution. *Tellus*, **51**, 373-386.

Kessler, W. and R. Kleeman, 2000: Rectification of the Madden-Julian Oscillation into the ENSO cycle. *J. Climate*, **13**, 3560-3575.Knutson, T. and K. Weickmann, 1987: 30-60 day atmospheric oscillations: Composite life cycles of convection and circulation anomalies. *Mon. Wea. Rev*., **115**, 1407-1436.

Madden R. and P. Julian, 1971: Detection of a 40-50 day oscillation in the zonal wind in the tropical Pacific, *J. Atmos. Sci*., **28**, 702-708.

Madden R. and P. Julian, 1972: Description of global-scale circulation cells in the tropics with a 40-50 day period. *J. Atmos. Sci*., **29**, 1109-1123.

Madden R. and P. Julian, 1994: Observations of the 40-50 day tropical oscillation: A review. *Mon. Wea.Rev*., 112-814-837.

Maloney E. and D. Hartmann, 2000a: Modulation of eastern North Pacific hurricanes by the Madden-Julian Oscillation, *J. Climate*, **13**,1451-1460.

Maloney E. and D. Hartmann, 2000b: Modulation of hurricane activity in the gulf of Mexico by the Madden-Julian Oscillation. *Science*, **287**, 2002-2004.

Matthews, A., B. Hoskins, J. Slingo, and M. Blackburn, 1996: Development of convection along the SPCZ within a madden-Julian oscillation. *Quar. J. Roy. Met. Soc*., **122**, 1473-1498.

Ogallo L and Nyakwanda W (1994): Spatial patterns of Outgoing Longwave Radiation over East Africa derived from rotational principal component.

Okoola R.E (1996): Space-time characteristics of ITCZ over equatorial East Africa during anomalous rainfall years. Ph.D Thesis, Department of meteorology, University of Nairobi, Kenya

Otieno F. O and E.A Anyamba(1994): OLR and SST characteristics during years of extreme rainfall over East Africa.

Omeny A.P (2006): East African rainfall variability associated with the Madden-Julian Oscillation. Msc.thesis , Department of meteorology, University of Nairobi, Kenya

Rui, H. and B. Wang, 1990: Development characteristics and dynamic structure of tropical intraseasonal convection anomalies, *J. Atmos. Sci.*, **47**, 357-379.

Zhang, C. and J. Gottschalck, 2002: SST anomalies of ENSO and the Madden-Julian Oscillation in the equatorial Pacific. *J. Climate*, **15**, 2429-2445.

Zhang, C. 2005: Madden-Julian Oscillation. *Reviews of Geophysics*, **43**, 1-36.

.